United States Progress on Nuclear Propulsion for Rockets

by

Harold B. Finger

Manager, Space Nuclear Propulsion Office
Atomic Energy Commission
and
National Aeronautics and Space Administration
USA

Presentation to

XVIIth International Astronautical Congress

Madrid, Spain

October 13, 1966

A major advance in rocketry has been achieved in the United States program to develop nuclear propulsion. The program to develop nuclear propelled rockets has experimentally demonstrated altitude specific impulse of more than 760 seconds assuming a nozzle area ratio of 40 to 1. An operating time of 30 minutes has been experimentally achieved at this specific impulse and full design power of 1100 megawatts. The ability to restart these systems and run them back up to full specific impulse and full power has been demonstrated. Stable operation has been achieved over a wide thrust range at this high specific impulse. The ability to control the system over the entire operating range from start-up to full power and during shutdown has been demonstrated with liquid hydrogen as the propellant. Reactor and total rocket system weight

is within a value that can permit large payload gains for many space missions as a result of the high specific impulse achieved. All of the above performance and operating characteristics have been demonstrated in full-scale power reactor and breadboard engine tests. In addition, laboratory scale experiments indicate the potential ability to go to higher specific impulse and longer operating time with high thrust engines and higher power density reactors.

The United States program to develop nuclear propulsion for rockets started in 1955 at the Los Alamos Scientific Laboratory (LASL) operated for the United States Atomic Energy Commission by the University of California. Non-reactor portions of the work (hydrogen turbopumps, nozzles) were conducted under U.S. Air Force sponsorship until 1958 when the National Aeronautics and Space Administration was established by Act of Congress to conduct our aeronautical and space research and exploration activities. In 1958, therefore, responsibility for nuclear rocket propulsion systems was assigned to NASA; responsibility for development of the nuclear reactors for such rockets remained with the AEC. It was already apparent at that time that nuclear rockets could offer significant advantages for deep space, high payload exploration missions if their potentially high specific impulse could be achieved in a reasonable weight system. This high specific impulse has now been achieved experimentally and reasonable weights have been verified.

The first slide (Fig. 1, R63-1294) shows a schematic drawing of a nuclear rocket engine with its turbine-driven pump pumping hydrogen from the propellant tank through the walls of the jet nozzle to cool that component, through the reflector, and then through the reactor where it is heated to high temperature, 4000°R (1980°C) or higher. The jet velocity at these conditions with a 40:1 area ratio nozzle would be about 24,500 fps or a specific impulse of over 760 seconds.

The major emphasis in the U.S. program has been on development of graphite reactors for such systems. The laboratory work at LASL led to the first reactor test in 1959 on the so-called KIWI-A reactor designed for 100 MW thermal energy (Fig. 2, RN62-885). The three reactors of this family that were tested were followed by tests of several designs of the KIWI-B reactors designed for about 1100 MW. These tests included the first test of a reactor with liquid hydrogen in September, 1962 (which showed that reactor control was possible even with this good neutron moderator as a reactor coolant), and led to the test of the KIWI-B4A reactor in November, 1962 (Fig. 3, R63-739B). This reactor was of a preferred design, but fuel element damage that occurred during the test revealed a significant flow and pressure induced vibration problem. The problem showed up during the test as flashes of light in the exhaust, which were actually incandescent particles of graphite. The following short movie of the test shows the appearance of the hydrogen exhaust jet during the test.

Obviously, this problem had to be solved before further power testing could be resumed. As a result, the year 1963 was devoted to component and subsystem tests that were designed to simulate, as well as possible, the operating conditions in the reactor but without generating nuclear power. These laboratory tests included hot gas flow tests of single fuel elements, cold flow tests of sections of the reactor, vibration tests of reactor parts and of the entire reactor assembly, etc.

Power testing of reactors was finally resumed in May, 1964, almost a year and a half after the November, 1962 KIWI-B4A reactor test had revealed the vibration problems in the design. Since May, 1964 we have conducted the tests shown on the next slide (Fig. 4, NPO65-2079) on seven KIWI and NERVA reactors and one breadboard engine system (NRX-EST). One reactor test (KIWI-TNT) was conducted to obtain data required in safety analyses to provide assurance of the safe operation of such systems. To better define these names given to our reactors, the KIWI reactors were named after the non-flyable New Zealand bird because they were intended as research and experimental reactors. By contrast, NERVA stands for Nuclear Engine for Rocket Vehicle Application.

All of these reactors are basically the same design. They are made up of clusters of graphite fuel elements through which the hydrogen propellant or coolant is passed. The fissionable material in these fuel elements is in the form of pyrolytic carbon coated particles of uranium

carbide. The flow passages in the fuel elements are coated with niobium carbide to protect the graphite from the corrosive effect of the hydrogen coolant.

One important point shown on this chart is that several reactors have been run several times. For example, the KIWI-B4E reactor was tested twice. The NERVA reactor experiment, NRX-A2, was tested twice. The NRX-A3 reactor was tested three times at full power and the breadboard engine, NRX-EST (Engine System Test) was restarted many times during its test series. The high reliability and our good understanding of these systems is demonstrated by the fact that every one of these tests met or exceeded the test objectives that had been set.

The KIWI-B4D reactor, the first reactor that was operated after resumption of testing, demonstrated that we had solved the vibration problem that had halted our test operations on the KIWI-B4A reactor. All of these following tests confirmed that the vibration problem had been solved by redesign of the reactor supporting structure.

The experience we have accumulated is illustrated in the next slide (Fig. 5, NPO65-1927) by the growth in operating time at design power during our test operations. As you can see, we have now operated for a total time at full power of close to two hours. The total operating time at power has been over four hours.

To bring you up-to-date on the current status of our nuclear rocket development, I would like to describe one of our most significant

series of tests - the NRX-EST (NERVA Reactor Experiment-Engine System Test) series.

With the exception of the breadboard engine, NRX-EST, all of our reactor tests were run in a configuration shown by the schematic drawing on the next slide (Fig. 6, NPO65-2117a). The reactor is shown mounted on a railroad car with a jet nozzle pointing upward to simplify the facility installation. The railroad car is moved by a remotely controlled locomotive so that it may be easily detached from the test cell after test operations. Hydrogen is provided to the reactor from large vacuum jacketed storage bottles, or dewars, by a facility turbopump that is driven by high pressure hydrogen gas stored at pressures up to 3600 psi. The hydrogen capacity in our test facilities is about 150,000 gallons in one test cell and over one million gallons in our other reactor test cell.

This test installation was modified only slightly to permit breadboard engine tests. The breadboard engine installation differs from the reactor tests, as shown in Figure 7 (NPO65-2117b) in that the turbopump is mounted directly on the railroad car beside the reactor and the turbine is driven by hot gas drawn from the reactor discharge through a bleed port in the jet nozzle. The facility high pressure gaseous hydrogen storage and the facility turbopump were bypassed during the engine system test. The hot hydrogen drawn from the nozzle bleed port to drive the turbine was diluted with cold hydrogen

drawn from the pressure vessel dome to reduce the turbine inlet temperature to about 1200°R (400°C). The flow to the turbine and, therefore, the speed of the turbopump were controlled by adjusting the position of the turbine power control valve using a pneumatic actuator. This test installation is essentially the same in its operation as is a nuclear rocket flight engine except that the components are not located as they would be in a flight installation. But all the components of an engine that permit the engine to start itself and sustain power operation are included.

The next figure (Fig. 8, NPO65-1915) shows a photograph of the breadboard engine installed at the test cell. The reactor is shown on top of the shielded compartment in which the reactor control drum actuators are located. The compartment to the left houses the turbopump, the turbine control valve, and other related components. A photograph of the inside of this enclosure showing the turbopump and the turbine power control valve is shown in the next slide (Fig. 9, NPO66-15616). This entire compartment was shielded so as to eliminate the need to fully qualify these components against nuclear radiation effects.

The pump used in this breadboard engine system test (EST) is shown in the next slide (Fig. 10, NPO64-669). It is a centrifugal pump driven by a two-stage turbine. It delivers more than 70 pounds per second of hydrogen and has hydrogen cooled and lubricated bearings.

The jet nozzle used in these tests is shown in Figure 11 (NPO66-328). Except for the addition of the hot bleed port through which hot hydrogen was drawn to drive the turbine, this nozzle is the same as the one that was used in previous NERVA reactor experiments. The nozzle is made of stainless steel coolant channels brazed into a forged stainless steel pressure shell.

The breadboard engine was controlled automatically during its operation using several different control modes. The control system used is indicated schematically in the next slide (Fig. 12, NPO66-15297). Engine control is achieved through regulation of two components. The reactor control drums, located in the reflector region around the reactor core, control neutron power. The neutron power level in turn affects reactor temperature and nozzle chamber or reactor discharge pressure. The other control component is the turbine power control valve which regulates the flow of gas driving the turbine, thereby affecting the turbopump rotational speed, the hydrogen flow rate, and the pump head. Various combinations of control loops and sensors were investigated. Tests were run with both closed loop control and open loop control. As an example, the control drums were set at a predetermined position and the turbine control valve was adjusted to increase hydrogen flow rate into the reactor thereby increasing reactor power to the design point.

Ten separate power tests were run on this breadboard system extending from February 3, 1966 to March 25. Figure 13 (NPO66-15342)

presents a summary of the power tests run on these systems and indicates the variety of control modes used and the variety of operating conditions investigated. Of these ten tests, four were run for a total of 28 minutes at full power conditions. The total power operating time on this engine system was 110 minutes with the power varied during these tests from 160 megawatts to 1130 megawatts. The maximum exhaust gas temperature achieved during the tests was 4175°R (2050°C).

These tests proved that the system could start on its own power. In all of our starts, the engine used the energy available in the pressurized propellant tank and the reactor heat to provide the starting energy. No external source of starting energy was provided.

The self-starting capability of these engine systems had been investigated in advance of the powered engine system tests with cold flow system tests. In such cold flow systems, which generate no fission energy, starting energy is provided by the pressure in the propellant tank and the ambient heat capacity of the reactor system. Obviously, good simulation of engine start conditions in these cold flow systems is limited to the first several seconds of startup during which time the temperature of the reactor is rapidly decreased, thereby eliminating the heat capacity source of energy. Comparison of the acceleration characteristics of the cold flow development test system (CFTDS) and the powered engine system tests is presented in Figure 14 (NPO66-15296). The CFTDS turbopump acceleration curves are shown as dotted lines and

the NRX/EST turbopump speed variations are shown as the solid lines. In general, the data in this figure indicate good agreement between the CFDTS and the EST during the start phase of the operation. Satisfactory acceleration of the turbopump is shown for the higher tank pressure conditions. However, it should be remembered that all of these tests were run at atmospheric exhaust pressure conditions in Nevada (12.7 psi). At space vacuum exhaust conditions the tank pressure required for satisfactory turbopump acceleration would be significantly reduced. A detailed evaluation of these start transients requires further operation with vacuum exhaust conditions simulating altitude start operations. Such data will have to come from engine tests in our engine test stands which I will describe briefly later in this presentation. However, the tests that have already been run, combined with our analytical methods, clearly demonstrate the self-start capability of nuclear rocket engines over a wide range of start conditions.

The wide range of operation of these nuclear rocket systems is illustrated in the next slide (Fig. 15, NPO66-15299). In this figure, I have presented the nozzle chamber temperature, which is the temperature at the reactor outlet, as the ordinate. This temperature, combined with the pressure ratio across the nozzle, or the nozzle area ratio, determines the specific impulse of these nuclear rocket systems. This chamber temperature is plotted against the nozzle chamber pressure or reactor discharge pressure, which is related to the thrust of these systems. The

allowable operating map of these engine systems is determined by three boundary conditions. There is a reactor structural limit which is determined by allowable structural temperatures and flow or nozzle chamber pressure conditions; there is a maximum temperature limit determined by fuel material capabilities and primarily by the corrosion of fuel material by hydrogen; and there is a maximum chamber pressure condition determined by the maximum flow that can be passed through the turbine power control valve. The dotted line indicates a hydrogen neutronic effect which must be watched, but does not limit operation in the power range of interest.

The three green colored areas, numbered 1, 2, and 3, define those regions in which extensive data were taken during startup, intermediate power operation, and full power and temperature operation of the EST. The dark lines in the operating range define various control operating modes that were investigated. For example, the horizontal line at high temperature indicates the ability to throttle the breadboard engine from full thrust or full power to reduced power while maintaining high reactor temperature (about 4000°R or 1980°C) and therefore high specific impulse. Similarly, the operating range was mapped at 3500°R (1670°C) and 2500°R (1120°C). Operation at a fixed turbine power control valve setting with control drum variation of power was investigated as was operation at fixed control drum position with varying turbine power control valve setting. This wide stable operating range indicates the

variety of possible control modes and general insensitivity of nuclear rockets to mode of increase in thrust from start to full thrust conditions.

Another important achievement in all of our operations has been that the time to go from about 1 megawatt to full power can be kept to under a minute. This is an extremely short time in nuclear reactor practice. Further, the fact that the starts were done completely automatically was a major development step.

The next movie taken during one of the full power tests of the EST breadboard engine system test will help to show the operating characteristics and configuration of our power tests. The exhaust jet of hot hydrogen can be seen above the jet nozzle. The cleanliness of this jet contrasts noticeably with the flashes of light I showed earlier in the KIWI-B4A test run in November of 1962 and with the orange color of that flame, which indicated release of graphite and corrosion of graphite. In this movie, the exhaust jet is almost invisible since hydrogen burns with a colorless flame. This indicates also that corrosion is not a major factor in this test run. The black and white portions of the film are taken with infrared sensitive film in order to better define the hot jet than is possible in the natural color films. In addition to the main jet exhaust, you can see two other jets which are the turbine exhausts. In all cases, we ignite the hydrogen as it discharges; you can see the ignition flare. The full power duration of the EST tests was 28 minutes,

but I would like to repeat that the power operating time with this total system was almost two hours.

In addition to the long series of successful reactor tests that we have had since May of 1964, I believe that the success of this, our first engine test, indicates the high reliability of these systems and their developability using fairly conventional development test approaches. It is important to note that every component, with the exception of one actuator, operated well during this entire test program. The original turbine power control valve actuator was not suitable for long operation and a redesigned actuator, which was previously under development because of the anticipated limitation of the original design, was installed during the test program. All of the tests beyond the first two power runs were conducted after the new actuator was installed.

Following the breadboard Engine System Test series, another test series was run on a reactor alone in June of this year. A photograph of this NRX-A5 reactor is shown in the next slide (Fig. 16, NPO67-114). Its test installation is similar to the schematic description of the test facility I showed earlier for all of our reactor tests. It operated at full power for 30 minutes with an altitude specific impulse, assuming a 40:1 area ratio nozzle, of over 760 seconds and an altitude equivalent thrust of 55,300 pounds.

A great deal of experimental data are now available. Using these experimentally determined reactor and breadboard engine data, we can

now more accurately analyze the benefits of nuclear rockets for application in possible future space exploration missions. It is important to emphasize that the nuclear rocket provides a basic increase in space propulsion capability. The missions that I will describe are, therefore, representative of a wide variety of potential future missions that could be performed with nuclear propelled rockets.

An important result of our mission analysis work has been the definition of a single NERVA engine that could perform all of the major missions for which nuclear rockets would offer significant advantages over chemical rockets. A drawing of this engine is shown on the next slide (Fig. 17, NPO67-49). It would be about 40 feet tall with a 80 or 100 to 1 nozzle area ratio and a reactor outside diameter of about 6 feet. It would have a power of about 5000 megawatts and give a thrust of 200,000 to 250,000 pounds. A specific impulse of 825 seconds should be readily achievable in the early versions of this engine based on the reactor temperatures we have already achieved.

We have further found from our mission analysis that this engine could be incorporated into a standard propulsion module, which is shown in Figure 18 (NPO65-1933). This module could also be used in all of the major nuclear rocket missions. It would have a diameter of 33 feet so that it could be installed as a third stage of the Saturn V chemical

booster rocket that is being developed by the United States as part of the manned lunar landing program. This module could be used singly or, for some of the missions I will describe, it could be clustered to provide the thrust required. Although the concept of a single propulsion module is not necessarily optimum for all missions, we have found that such a modular nuclear rocket would still provide major payload or total vehicle weight advantages. Further, we believe that the high reliability that would result from using a single system for all nuclear rocket applications and the reduced mission development costs strongly recommend this approach.

The next slide (Fig. 19, NPO65-1874) illustrates the mission versatility of this propulsion module. These various applications use the same basic propulsion module and would require development of only one basic set of subsystems: one engine model, one set of stage systems, one basic tank configuration. Our studies indicate that even though we would use the same hardware for all of these various missions, significant performance advantages would be provided by nuclear rockets; the payload would be increased significantly for manned planetary landings or flybys, manned lunar missions, and unmanned deep space probes. Thus, nuclear rockets can play an important role in a number of alternate routes which future space exploration may take.

It is generally apparent that the pay-off or advantages of nuclear propulsion will be greatest where the velocity increments for the mission are large, thereby increasing the advantage of high specific impulse and the resulting decrease in propellant loading. As a result, a good deal of our analysis has been devoted to planetary missions and specifically to Mars manned landing missions. A drawing of the orbital vehicle system that we have defined for such a manned Mars landing mission is shown on the next slide (Fig. 20, NPO67-242). This vehicle would be assembled in Earth orbit. It would be made up of a cluster of three nuclear rocket propulsion modules in the Earth orbit departure stage, a single propulsion module in the Mars orbit arrival stage, and another single propulsion module in the Mars departure stage. The maximum operating time for these engines would be about 30 minutes, which is the time that we have already achieved in the ground tests that I described earlier.

The total weight of this manned Mars landing space vehicle system is presented in Figure 21 (NPO67-31). The initial weight of the spacecraft for such a mission established in Earth orbit is plotted against launch year for the straightforward, all-propulsive mode in which nuclear rocket propulsion is used for Earth-orbit departure, Mars-orbit establishment and Mars-orbit departure. Chemical propulsion is used for landing on the planet, return to the orbiting spacecraft and retro at Earth return. Also shown are the

Earth orbit weights if atmospheric braking is used to decelerate the spacecraft at Earth return. The dark rectangles indicate the vehicle weight that would be required in Earth orbit for the Venus swingby trajectory in which the assistance of the Venus gravitational attraction could be used in the mission. The figure shows that variations from one mode to another and over the cycle of launch opportunities result in a range of initial space vehicle weights required in Earth orbit of 1.5 to almost 3 million pounds with nuclear rocket propulsion. Chemically propelled spacecraft would weigh two to four times as much, so millions of pounds of additional weight would have to be carried to Earth orbit if chemical propulsion systems were to be considered for such missions.

Considering the uncertainties involved in carrying out such a mission that may be 15 to 20 years off, our work is aimed at providing a propulsion capability for the most difficult mission times and mission modes. As a result, the approaches we are working on could also be used for Venus landing missions if such missions proved desirable.

Another manned planetary mission which may find a place in future space exploration is a flyby of Mars or Venus. Flyby missions may precede manned landings on these planets. A single nuclear rocket propulsion module, as illustrated in Figure 22 (NPO65-1876) could perform such flyby missions with rendezvous in Earth orbit of two Saturn V payloads. The weight in Earth orbit required to do

these flyby missions with nuclear propulsion is compared with chemical propulsion in the next slide (Fig. 23, NPO67-33). The number of Saturn V launches required to place the required weight in Earth orbit is also shown. Large savings in weight and in mission costs are apparent.

The same 33 foot diameter, 200,000 to 250,000 pound thrust nuclear rocket propulsion module could also be used as a third stage on our Saturn V launch vehicle in a configuration such as that drawn in the next slide (Fig. 24, NPO67-19). Such a nuclear Saturn V could be used for direct flight lunar missions, unmanned planetary orbiters and planetary probes, close-in solar probes, etc.

The payload that could be landed directly on the moon, without first going into a lunar orbit by such a nuclear Saturn V vehicle using a chemical cryogenic lunar landing stage, is compared in the next slide (Fig. 25, NPO67-29) with the payload of all-chemical combustion Saturn V vehicles. Saturn V vehicles with different potential amounts of uprating are shown. In all cases, the nuclear third stage provides a significant payload increase (65 to 85 percent) over the all-chemical vehicles.

This same nuclear Saturn V vehicle could also be used for unmanned probes throughout the solar system. The next slide (Fig. 26, NPO67-28) compares the nuclear Saturn V payloads with those of the

all-chemical Saturn V vehicles. Again, increases of 90 to 125 percent are possible by using the nuclear stage.

I would like to reemphasize that all of these missions I have described would use the 200,000 to 250,000 pound thrust NERVA powered propulsion module I described earlier. Obviously, this single system is versatile in mission application and would provide a basic and major increase in our space mission capability.

We have indeed made major progress in this program; it gives us confidence in our ability to develop nuclear propulsion for any of the many missions we have analyzed. The program that we have planned and that we will be conducting during the next few years will answer our remaining technological questions. Additional reactor tests are planned. They are aimed at achieving full power operating times even longer than the half hour we have already achieved. In addition, we will be testing the so-called Phoebus reactors aimed at establishing the technology of the 5000 megawatt, high power density reactors that will be needed in the versatile nuclear propulsion module I described. Tests of these larger reactors require the development of new jet nozzles. The nozzle that will be used with the Phoebus reactors is shown in the next slide, (Fig. 27, NPO67-37). It uses essentially the same design concept as the nozzle we used in the tests I described earlier, but it is significantly larger, as you can see from the comparison shown in the next slide (Fig. 28, NPO65-2107).

In addition, we are now preparing for tests of our Ground Experimental Engine shown in the next slide (Fig. 29, NPO67-143). This engine uses the 1100 megawatt reactor and essentially the same turbopump and jet nozzle used in our breadboard Engine System Test that I discussed earlier. The engine is built in three major subsystems so that a subsystem may be replaced using remote handling equipment if problems occur during tests in a component within one of these subsystems.

This engine will be tested in the Engine Test Stand, shown in Figure 30 (NPO67-48), which is now nearing completion. The exhaust duct shown here is now being checked out in the test stand. It includes a steam ejector that will permit engine test operations at altitude pressure conditions. It is built much like a jet nozzle in that it is internally cooled with water flowing through the flow passages that form its skin. The removal of a radioactively hot engine after testing from the test stand or reinstallation of such an engine into the test stand will be done remotely using the Engine Installation Vehicle and Manned Control Car shown in the next slide (Fig. 31, NPO67-47). Installation and removal can be done remotely under the control of a man located in the shielded cab of this locomotive.

Tests of the Ground Experimental Engine will provide additional data on the operating characteristics of nuclear rocket engines, but they will also give us experience and information on development test facilities and on handling and checkout of engines and facilities.

In conclusion, while preparing the complex spacecraft and chemical rocket vehicles that will land men on the moon, while providing important scientific data about the moon and the planets using unmanned spacecraft, while applying satellite technology for meteorological and communications systems, while investigating the role and operating capabilities of men and equipment in Earth orbit for long periods of time, the United States has also been looking ahead and has conducted work aimed at establishing the technologies that will be required to permit more extended exploration of space. As a result of this broadly based and farsighted program, we have now largely established and demonstrated the technology of nuclear propulsion for rockets. We have carried this work to the point that we now know we can achieve specific impulses of about 800 seconds for operating times that will be required of most space missions and our laboratory data indicate that we will be able to go to higher specific impulse with longer operating time with basically our present systems. We have now experimentally demonstrated the high performance that had been previously predicted for these systems. Although these nuclear propulsion systems provide their greatest payload and vehicle weight advantages for the very high energy, high payload missions, our analysis has shown that they are extremely versatile and it is for that reason they must be considered as a basic increase in space propulsion capabilities.

Further work is still to be done and is planned to extend the operating time for these graphite reactor systems, to increase the specific impulse to the higher levels that laboratory experiments indicate are realistically achievable, to the higher power and higher power density levels that appear to have the broadest space mission versatility, and to the demonstration of these systems in more nearly flight configured engines that operate in test stands with simulated altitude exhaust pressure conditions. This work, combined with the results of our extensive safety program, which I have not had time to discuss, permits us to look ahead to extensive space exploration with confidence that these systems can be developed for any performance that our mission analysis indicates is necessary and that they can be operated with high reliability and high assurance of safety.

LIST OF FIGURES

1.	Nuclear Rocket Engine	R 63-1294
2.	KIWI-A Reactor	RN 62-885
3.	KIWI-B4A Reactor	R 63-739B
4.	Graphite Reactor and Engine System Test Activities	NPO 65-2079 (9-1-66)
5.	Reactor Test Log	NPO 65-1927 (8-3-66)
6.	Reactor Test	NPO 65-2117a
7.	Breadboard Engine System Test (EST)	NPO 65-2117b
8.	Engine System Test (EST)	NPO 65-1915
9.	Engine System Test Propellant Fuel System Installation	NPO 66-15616
10.	NERVA/EST Turbopump	NPO 64-669
11.	Hot Bleed Port Nozzle-EST	NPO 66-328
12.	Nuclear Rocket Engine Control Schematic	NPO 66-15297
13.	EST Summary of Power Tests	NPO 66-15342
14.	Engine System Test Start Characteristics	NPO 66-15296
15.	EST Exploration of Operating Map	NPO 66-15299
16.	NRX-A5 Reactor	NPO 67-114
17.	NERVA Engine	NPO 67-49
18.	Propellant Module Concept	NPO 65-1933
19.	Versatility	NPO 65-1874
20.	Modular Nuclear Mars Vehicle	NPO 67-242

LIST OF FIGURES cont'd.

21.	Earth Orbit Weights for Mars Landing	NPO 67-31
22.	Flyby Vehicle	NPO 65-1876
23.	Flyby Weights	NPO 67-33
24.	Nuclear Saturn V	NPO 67-19
25.	Lunar Direct Landing Missions	NPO 67-29
26.	Unmanned Solar System Missions	NPO 67-28
27.	Phoebus Nozzle Photo	NPO 67-37
28.	Nozzle Compairson	NPO 65-2107
29.	Ground Experimental Engine (XE)	NPO 67-143 (9-27-66)
30.	Engine Test Stand-1 Exhaust Duct Installation in Progress	NPO 67-48
31.	Engine Remote Installation Equipment with Engine Mock up	NPO 67-47

GPO-913-247

PROPULSION MODULE CONCEPT

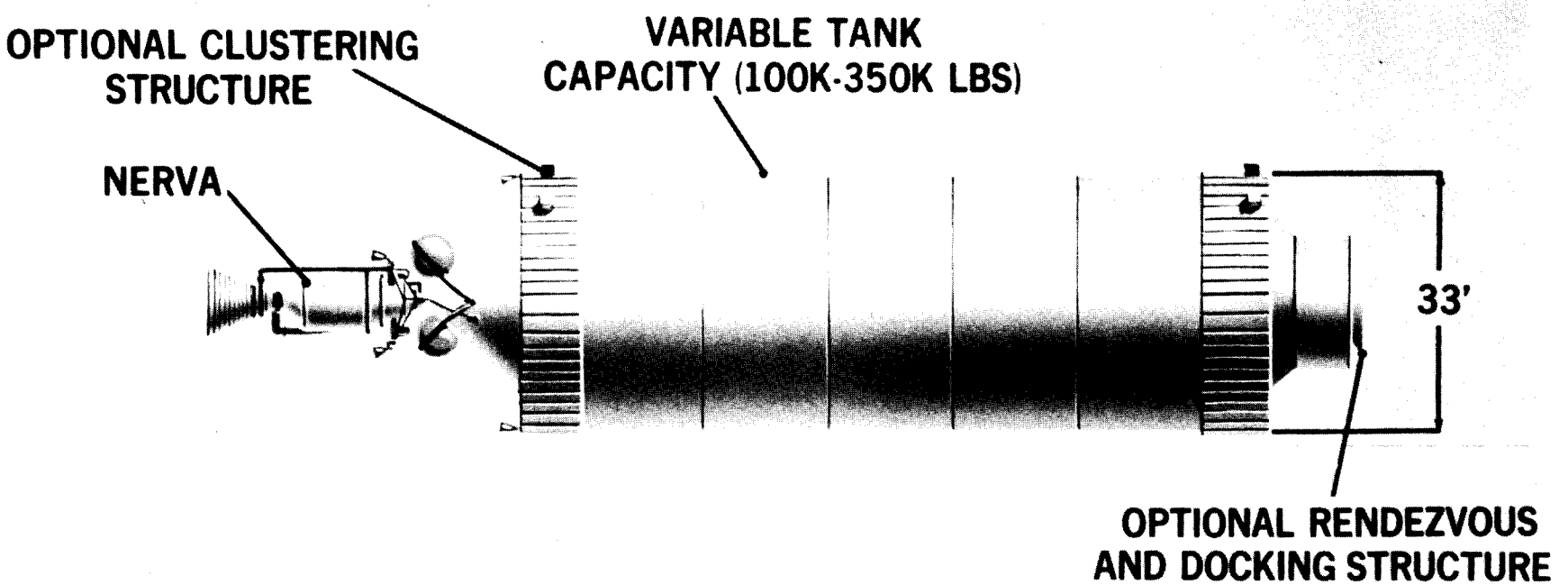

NASA NPO 65-1933
12-14-65

FIGURE 18

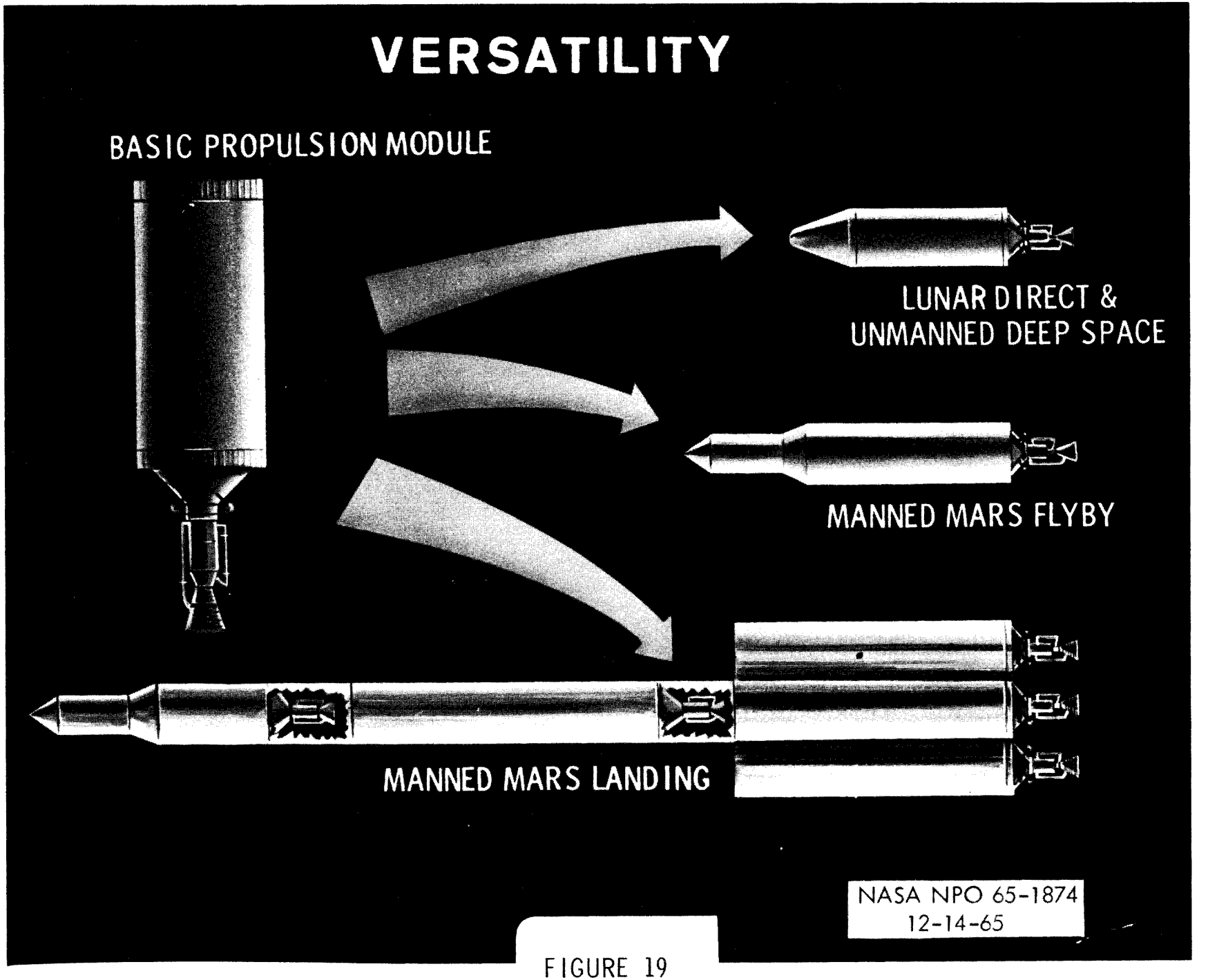
VERSATILITY
BASIC PROPULSION MODULE
LUNAR DIRECT &
UNMANNED DEEP SPACE
MANNED MARS FLYBY
MANNED MARS LANDING
NASA NPO 65-1874
12-14-65

FIGURE 19

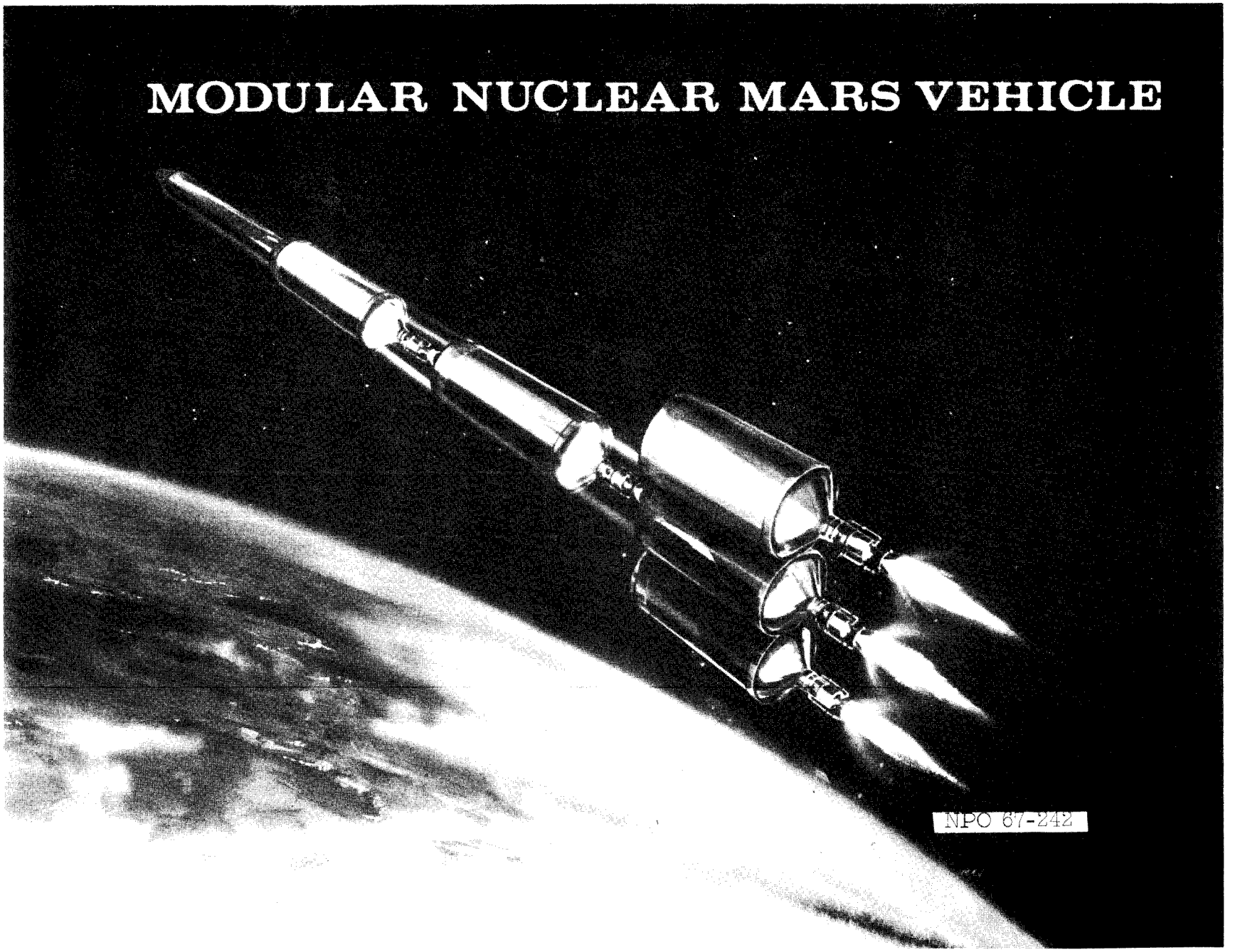

FIGURE 20

EARTH–ORBIT WEIGHTS FOR MANNED MARS MISSION

NUCLEAR ROCKET FOR EARTH DEPARTURE, MARS ARRIVAL, MARS DEPARTURE

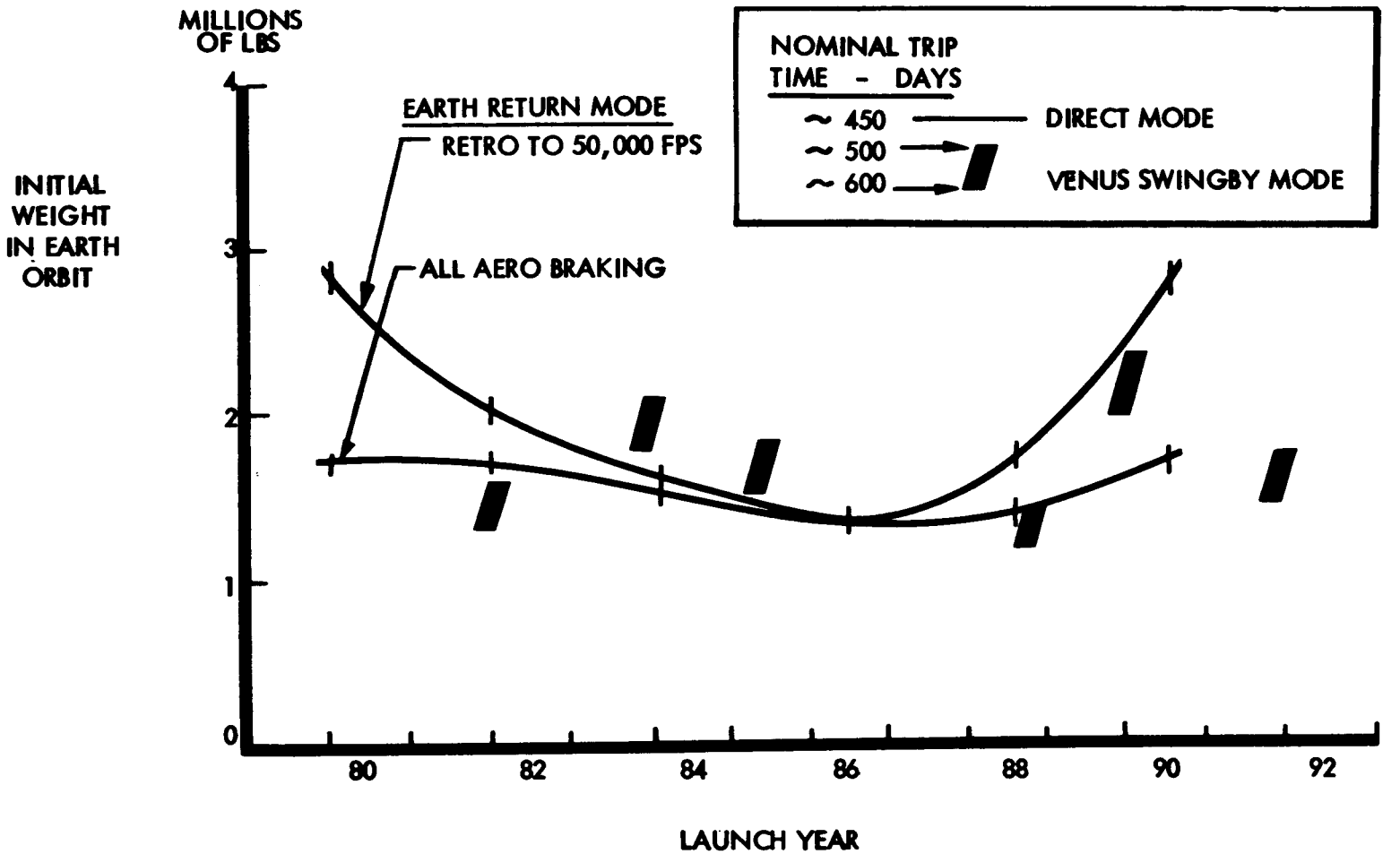

NASA NPO 67-31
9/27/66

FIGURE 21

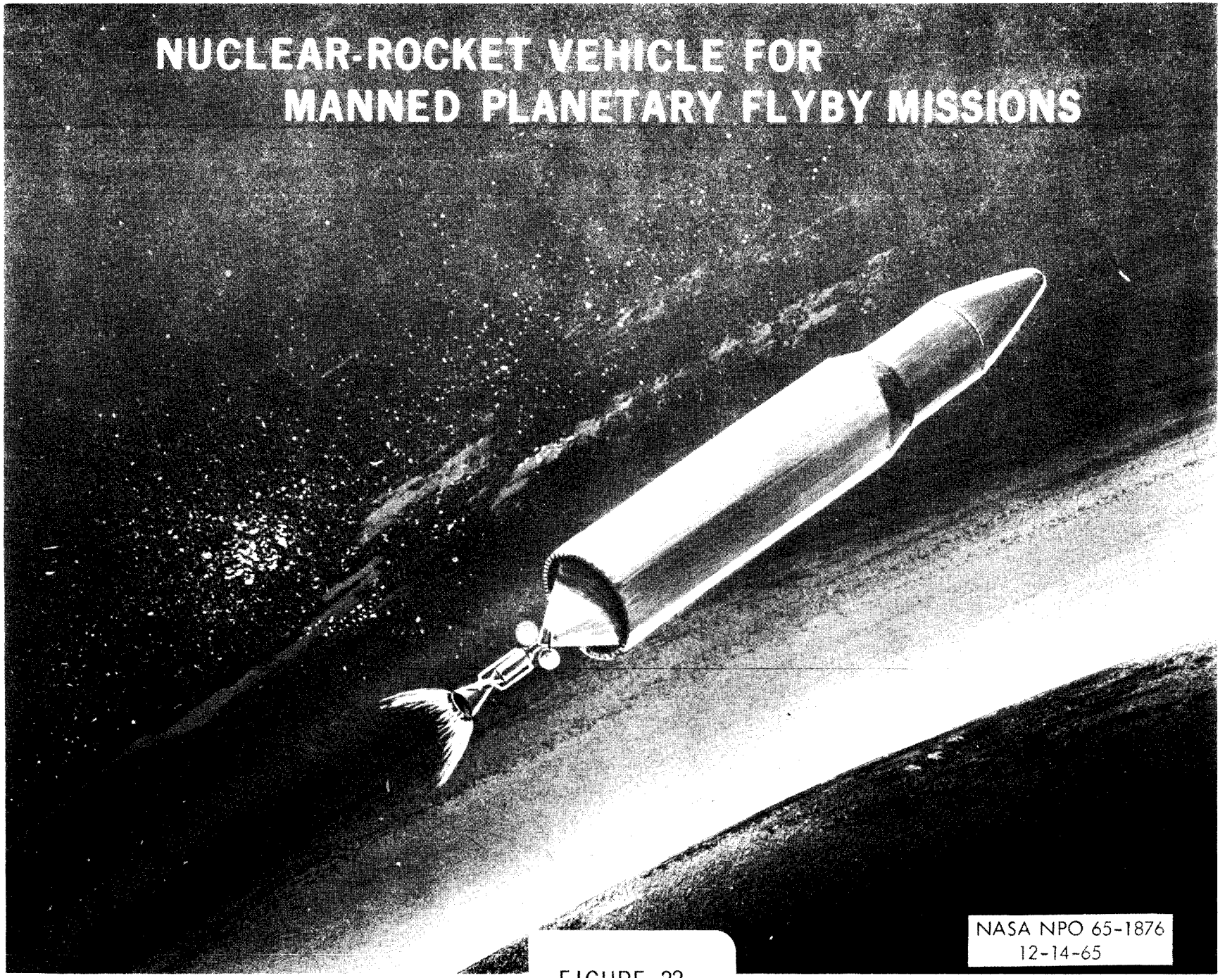
NUCLEAR-ROCKET VEHICLE FOR
MANNED PLANETARY FLYBY MISSIONS
NASA NPO 65-1876
12-14-65

FIGURE 22

EARTH ORBIT WEIGHTS FOR MANNED PLANETARY FLYBY MISSIONS

SPACECRAFT WEIGHT ≐ 180,000 LBS.

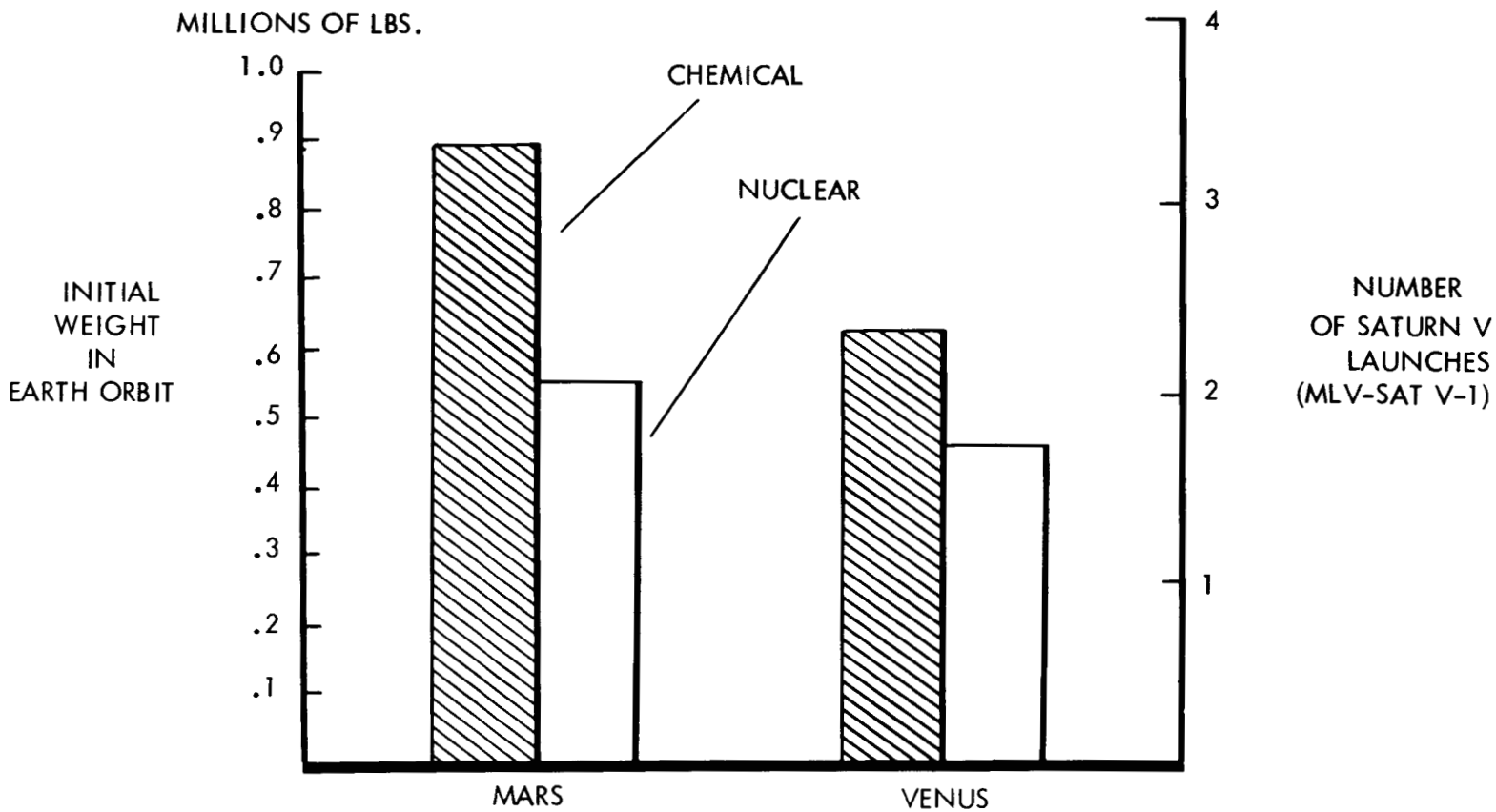

NASA NPO 67-33
9/27/66

FIGURE 23

NUCLEAR SATURN V

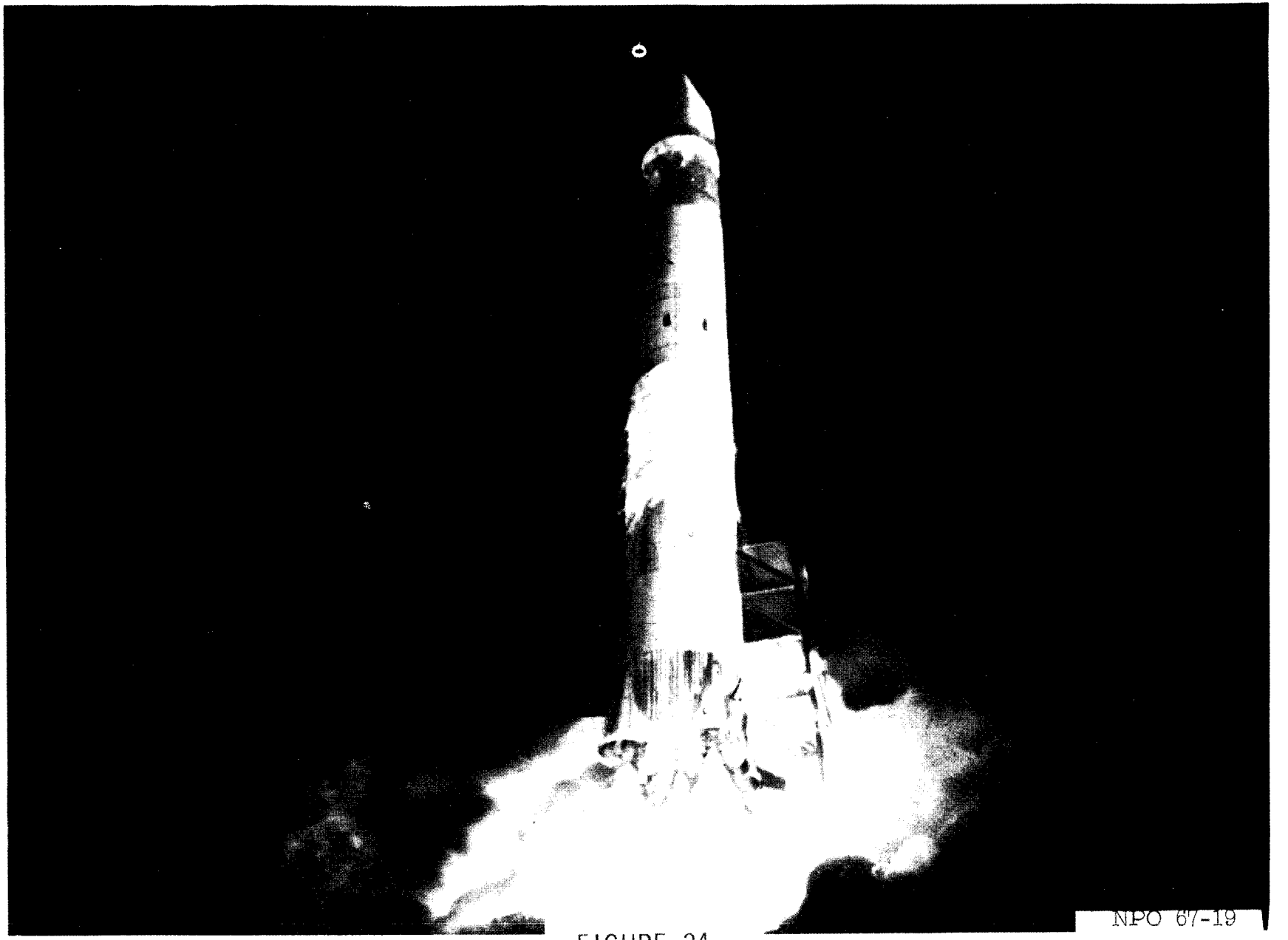

NPO 67-19

FIGURE 24

APPLICATION OF NUCLEAR THIRD STAGE TO SATURN V

LUNAR DIRECT-LANDING MISSIONS

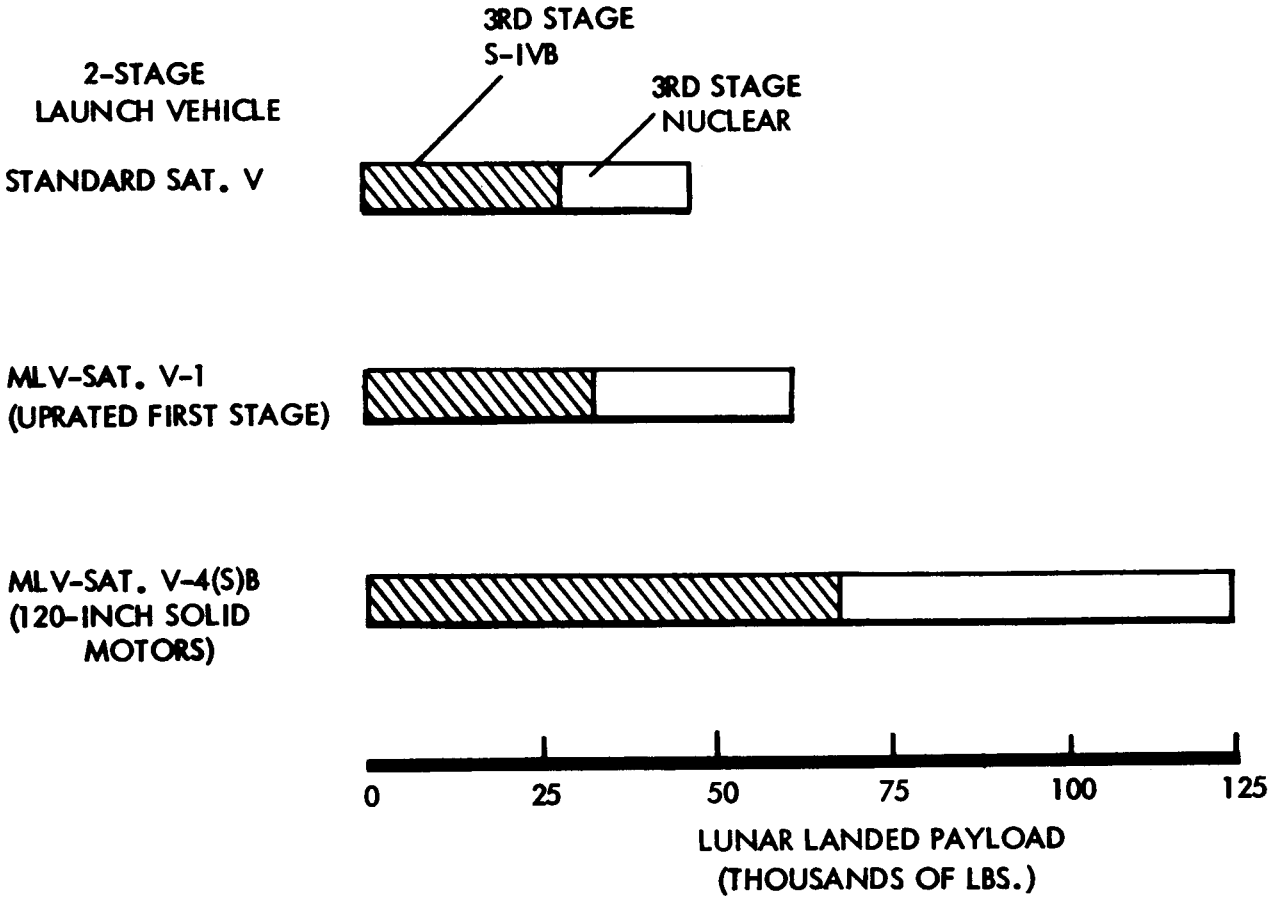

NASA NPO 67-29
9/27/66

FIGURE 25

APPLICATION OF NUCLEAR THIRD STAGE TO SATURN V

UNMANNED SOLAR SYSTEM MISSIONS

STANDARD SATURN V 1ST & 2ND STAGES

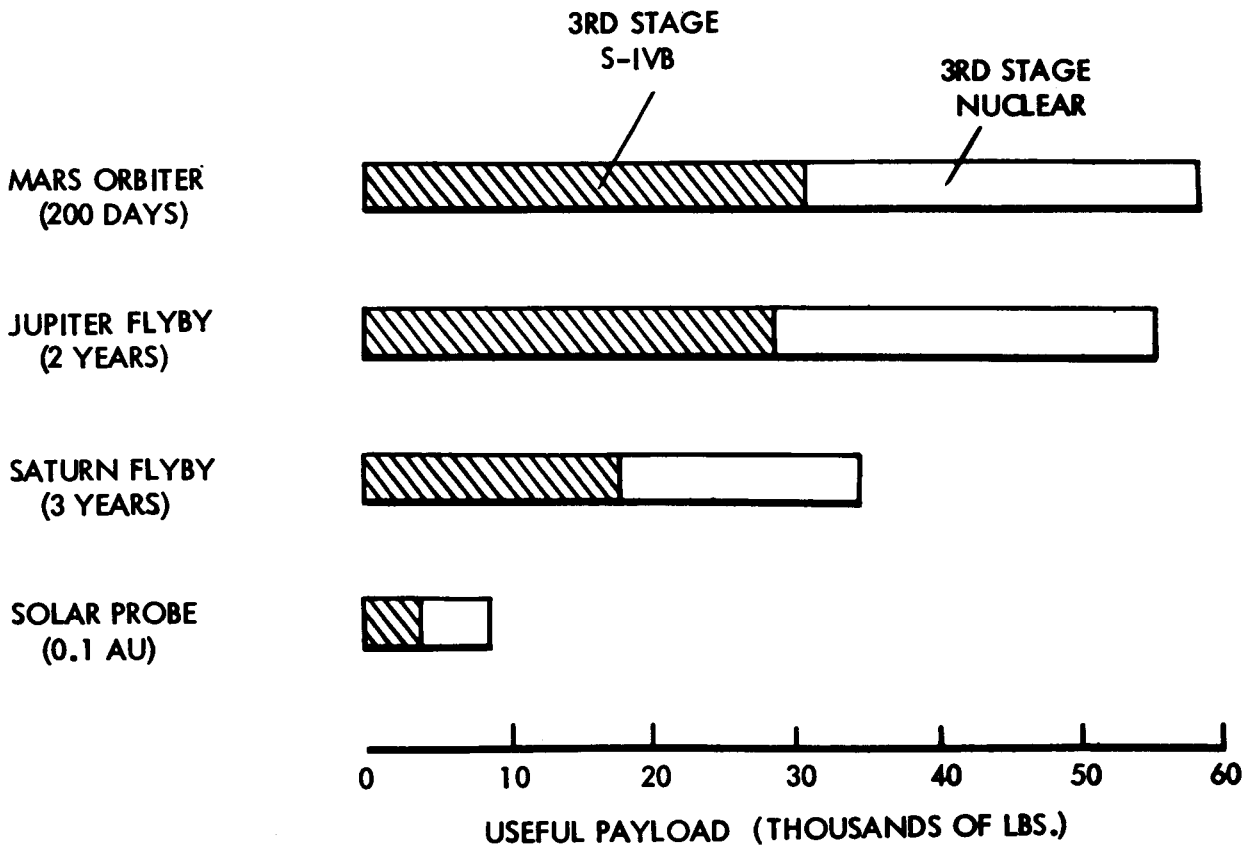

NASA NPO 67-28
9/27/66

FIGURE 26

FABRICATION TECHNOLOGY
PHOEBUS-2 NOZZLE

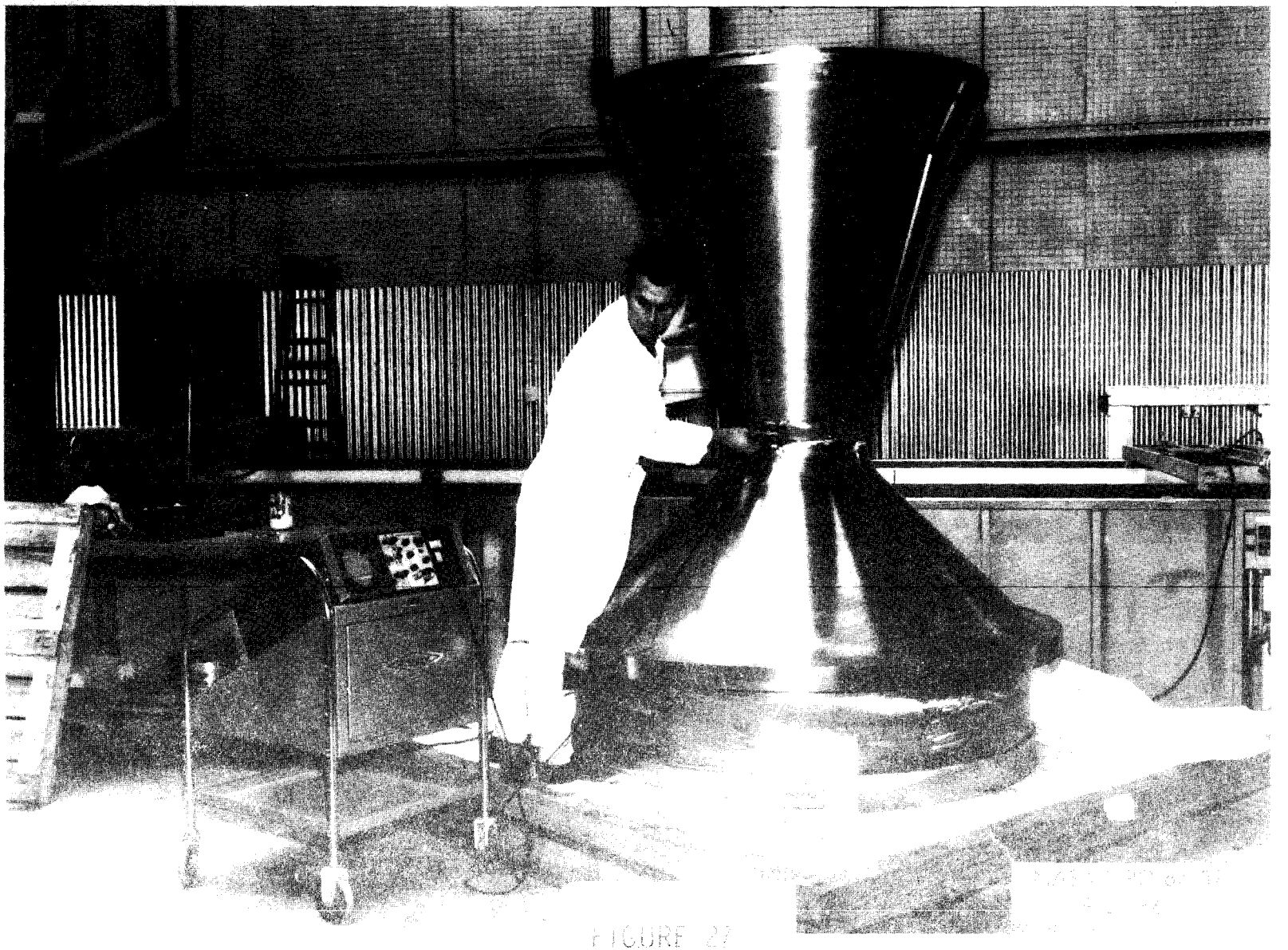

FIGURE 27

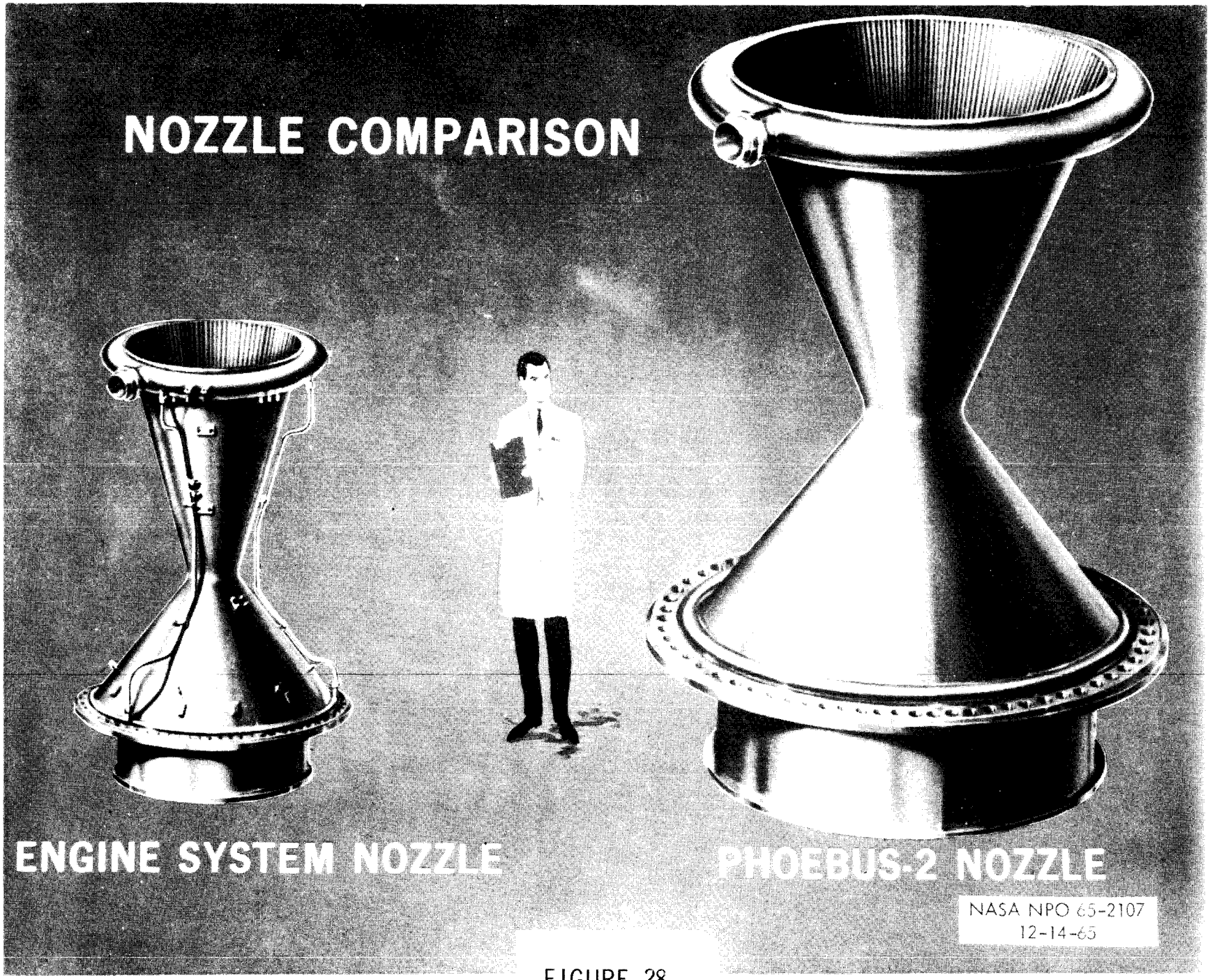
NOZZLE COMPARISON
ENGINE SYSTEM NOZZLE
PHOEBUS-2 NOZZLE
NASA NPO 65-2107
12-14-65

FIGURE 28

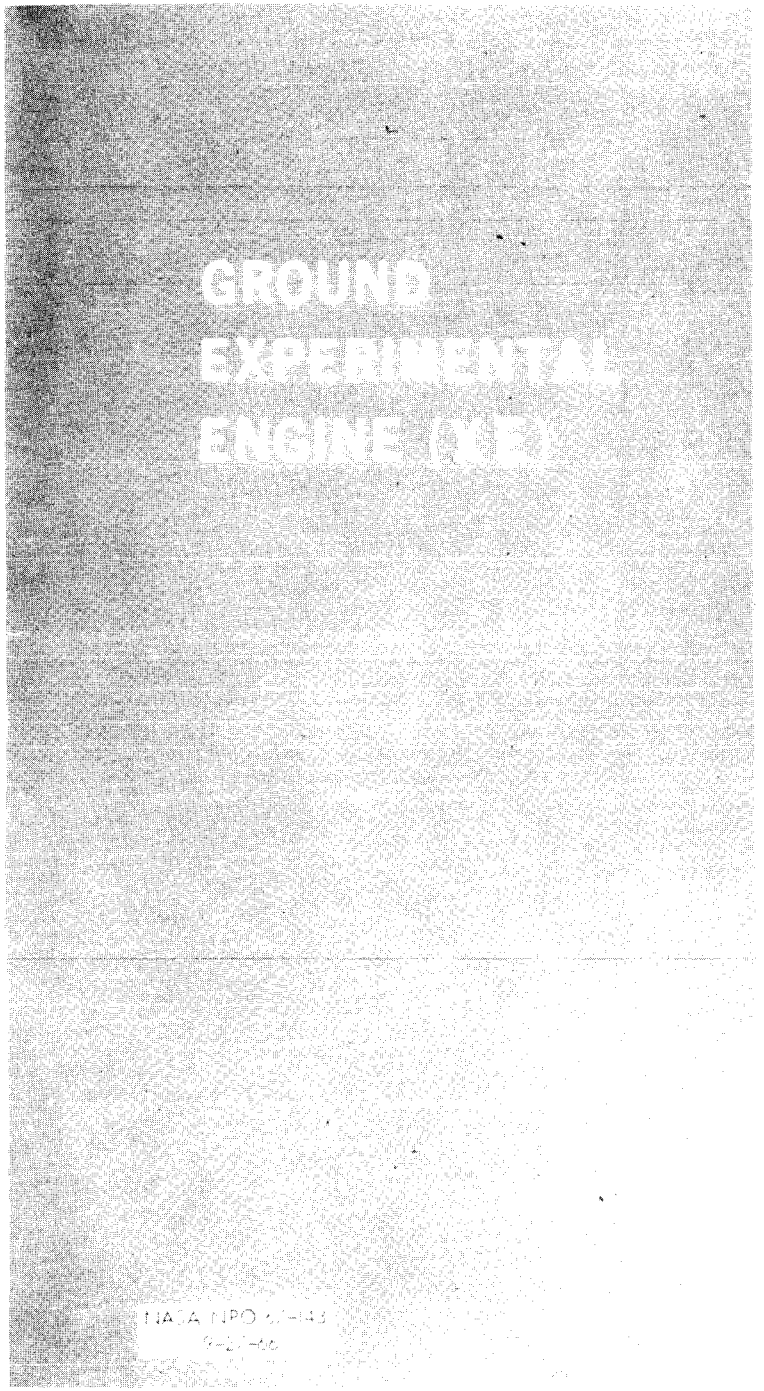
GROUND
EXPERIMENTAL
ENGINE (GE)

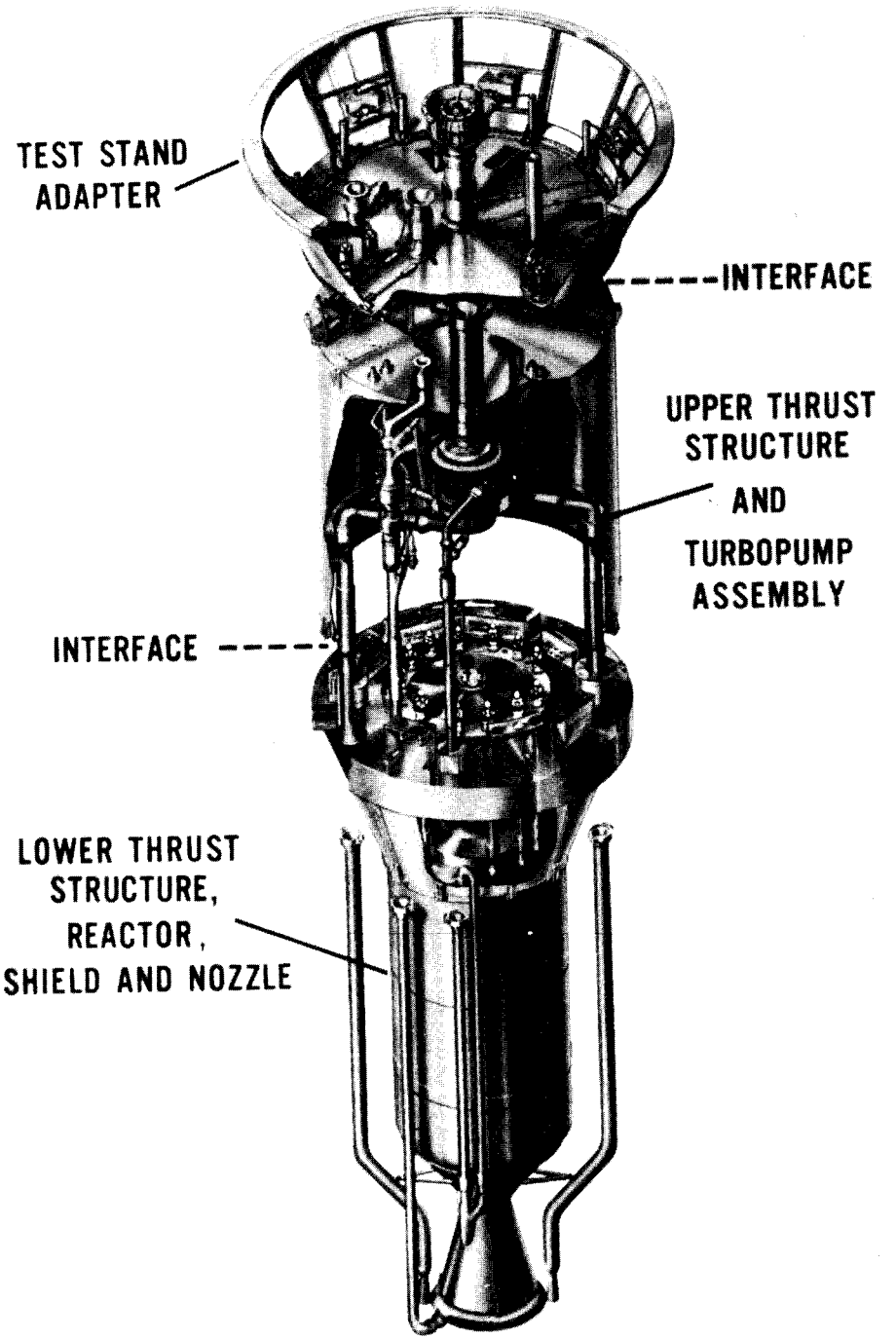
TEST STAND
ADAPTER
INTERFACE
UPPER THRUST
STRUCTURE
AND
TURBOPUMP
ASSEMBLY
INTERFACE
LOWER THRUST
STRUCTURE,
REACTOR,
SHIELD AND NOZZLE

FIGURE 29

ENGINE TEST STAND 1 EXHAUST DUCT INSTALLATION IN PROGRESS

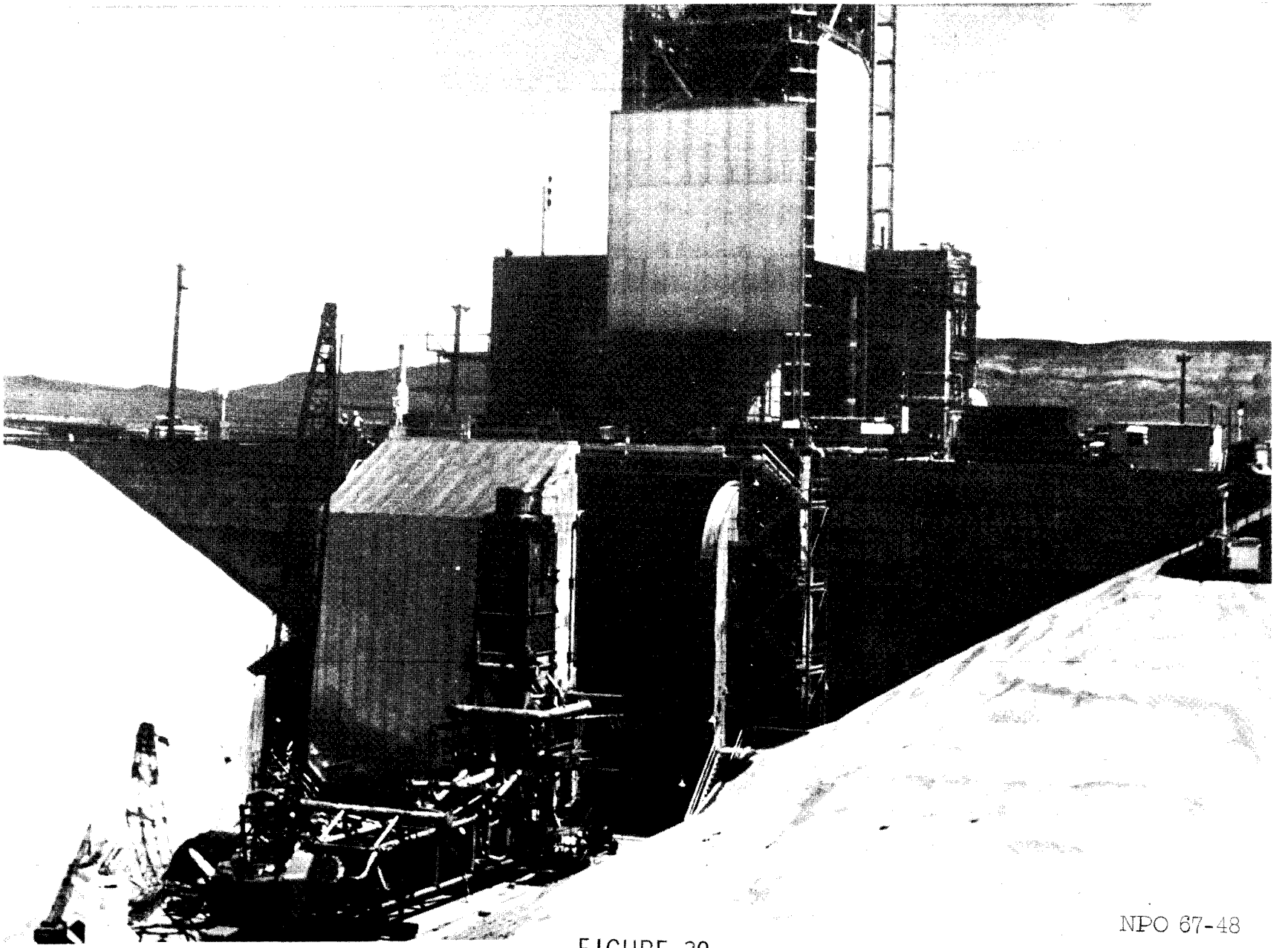

NPO 67-48

FIGURE 30

ENGINE REMOTE INSTALLATION EQUIPMENT WITH ENGINE MOCK UP

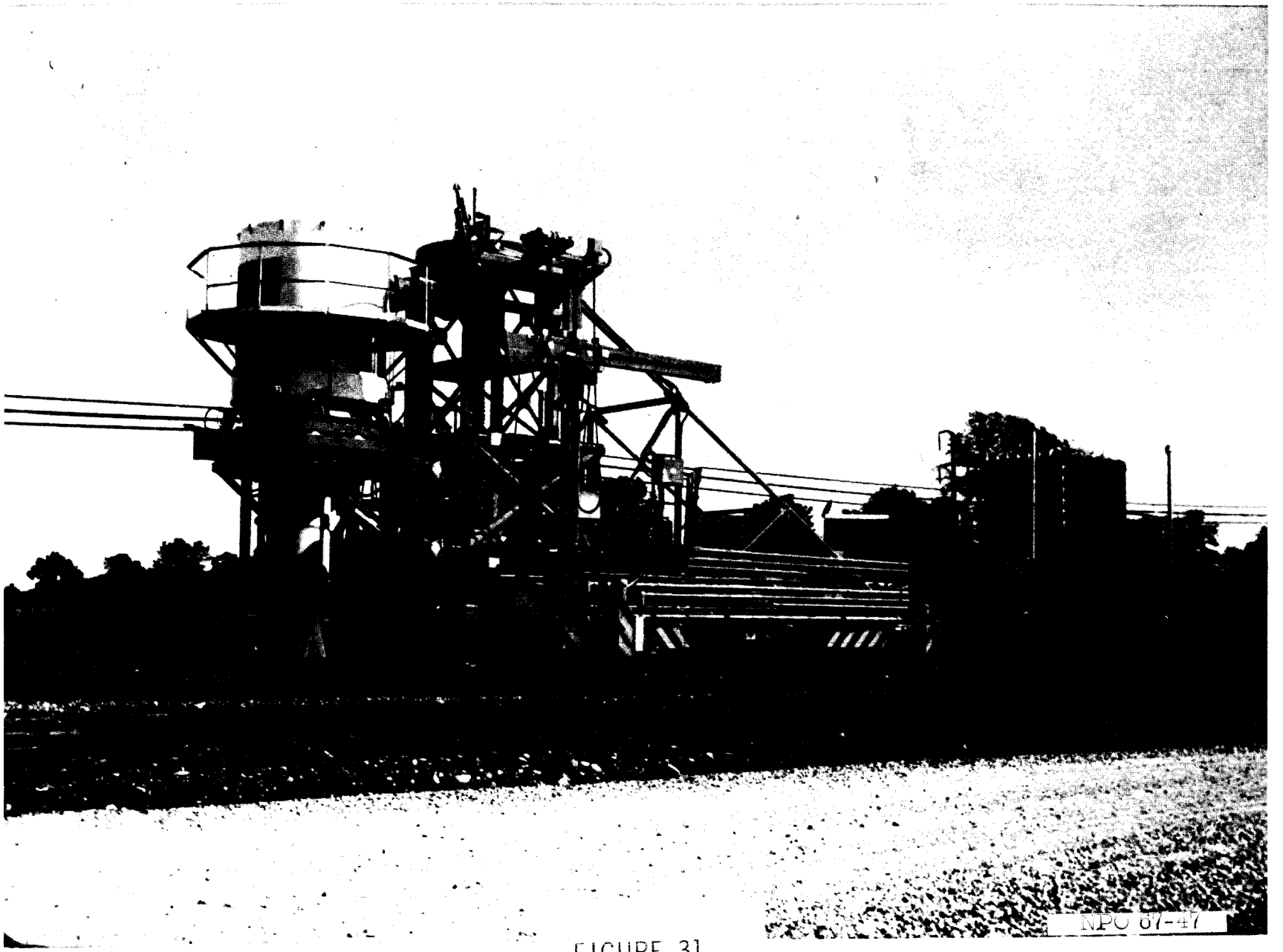

FIGURE 31

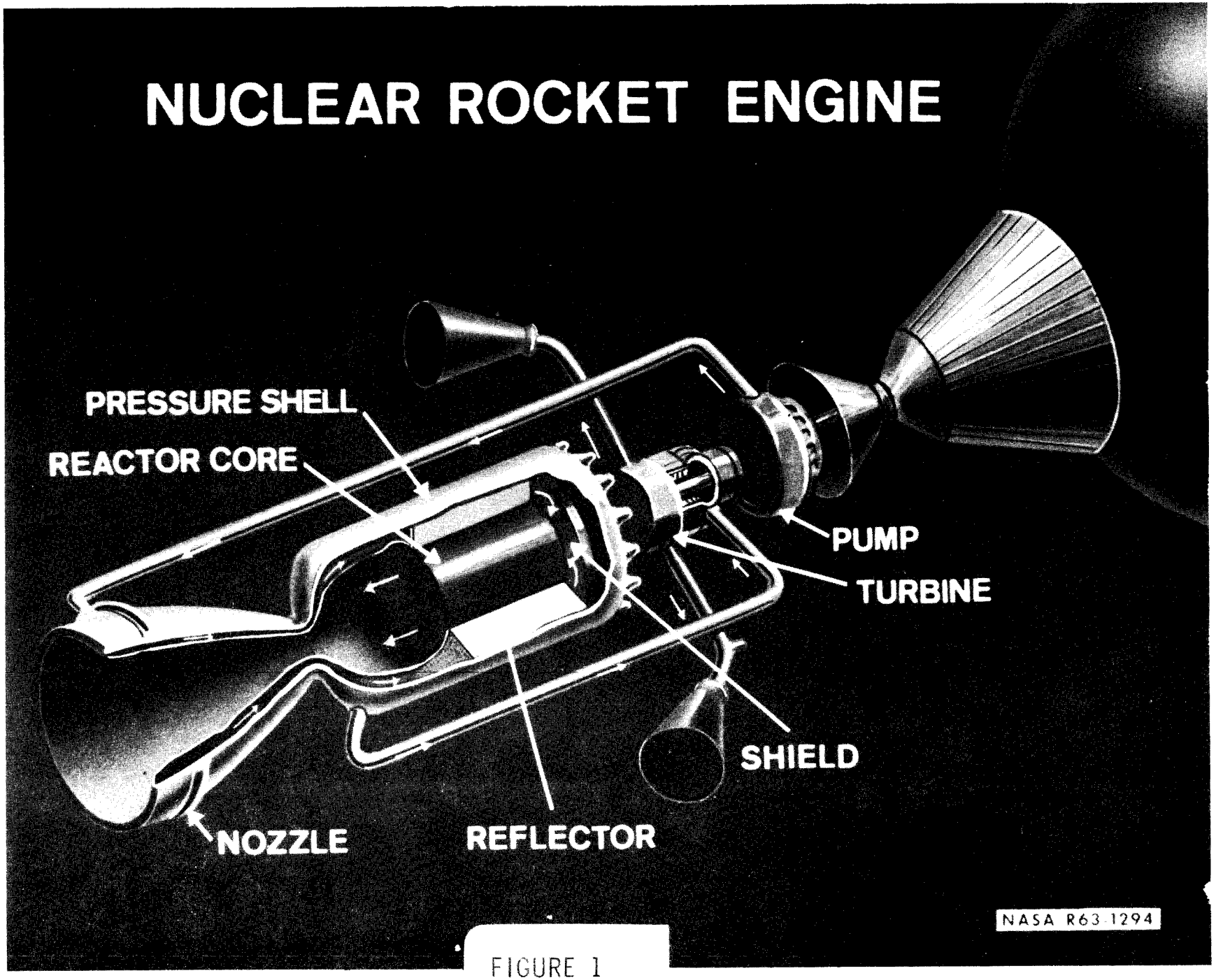
NUCLEAR ROCKET ENGINE
PRESSURE SHELL
REACTOR CORE
PUMP
TURBINE
SHIELD
NOZZLE
REFLECTOR
NASA R63-1294

FIGURE 1

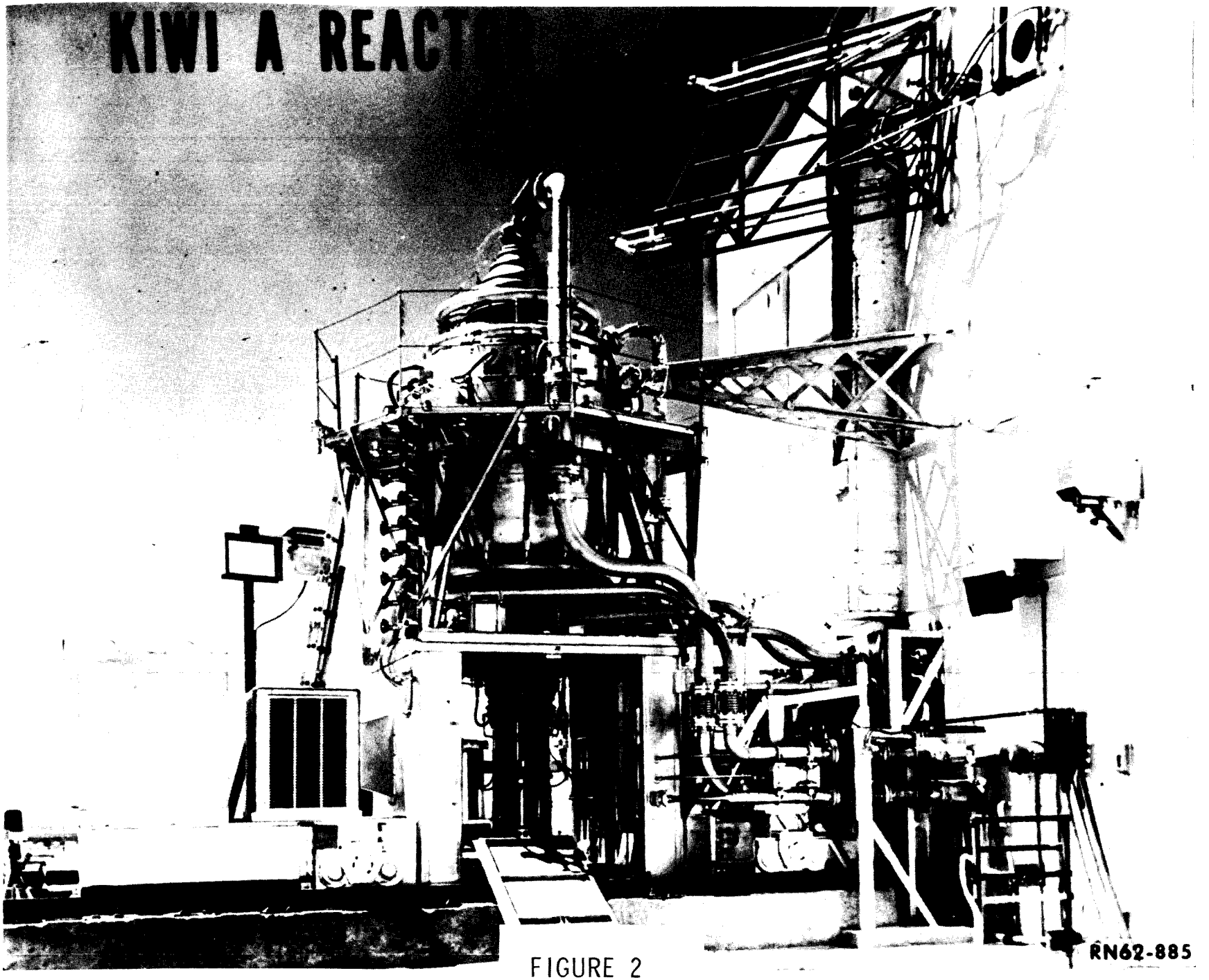

FIGURE 2

KIWI-B4-A REACTOR

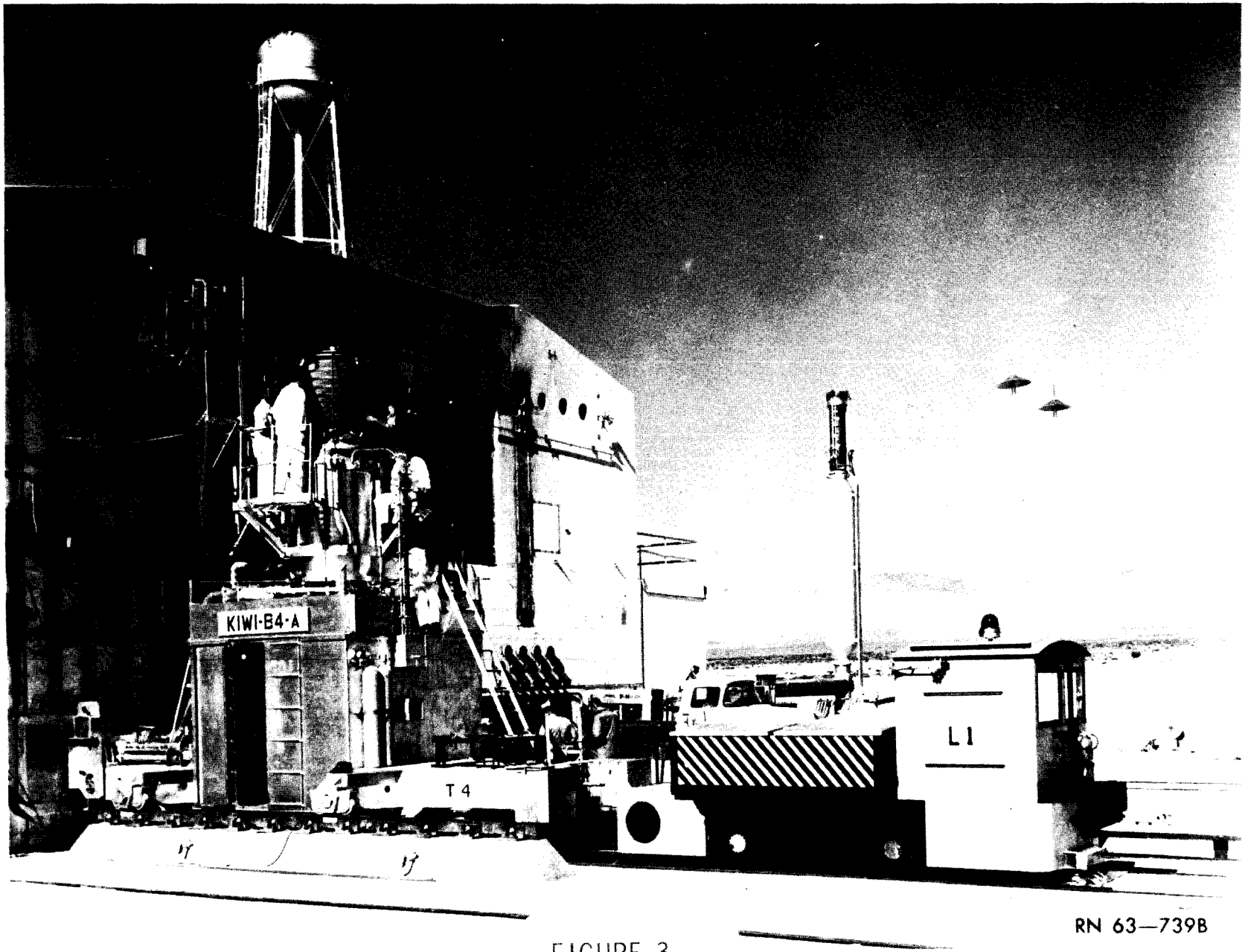

RN 63—739B

FIGURE 3

GRAPHITE REACTOR AND ENGINE SYSTEM
TEST ACTIVITIES

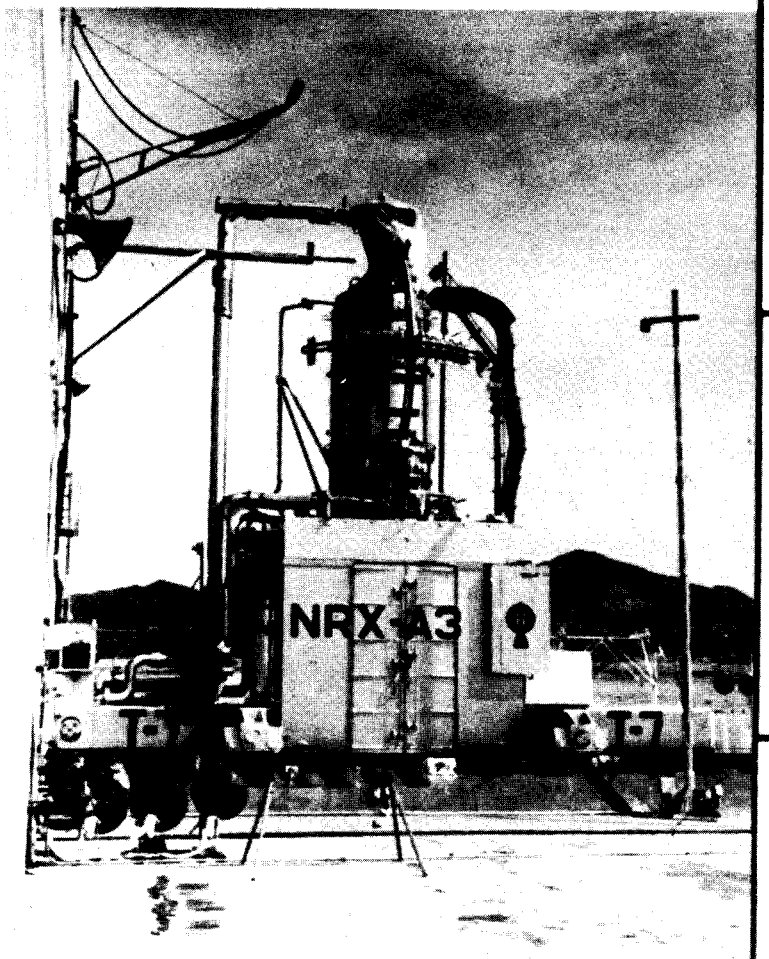

KIWI-B4D POWER	MAY 13, 1964
KIWI-B4E POWER	AUGUST 28, 1964
KIWI-B4E RESTART	SEPTEMBER 10, 1964
NRX-A2 POWER	SEPTEMBER 24, 1964
NRX-A2 RESTART	OCTOBER 15, 1964
KIWI TNT	JANUARY 12, 1965
NRX-A3 POWER	APRIL 23, 1965
NRX-A3 RESTART (1ST)	MAY 20, 1965
NRX-A3 RESTART (2ND)	MAY 28,1965
PHOEBUS-1A POWER	JUNE 25, 1965
NRX/EST (10 STARTS)	DEC. 1965-EARLY 1966
NRX-A5 POWER	JUNE 8, 1966
NRX-A5 RESTART	JUNE 23, 1966

FIGURE 4

NUCLEAR-ROCKET PROGRAM TEST LOG

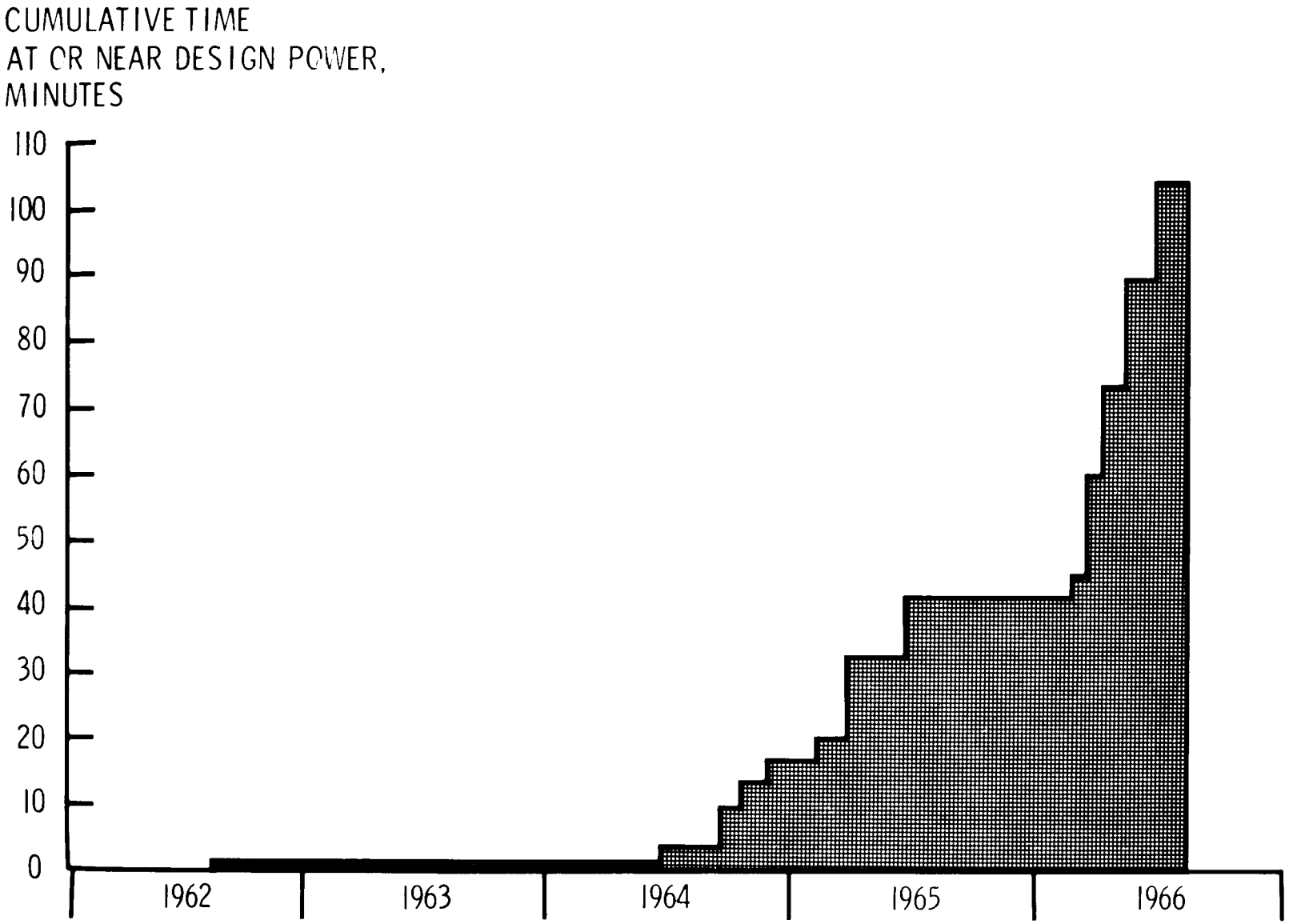

NASA NPO 65-1927
Rev. 8-31-66

FIGURE 5

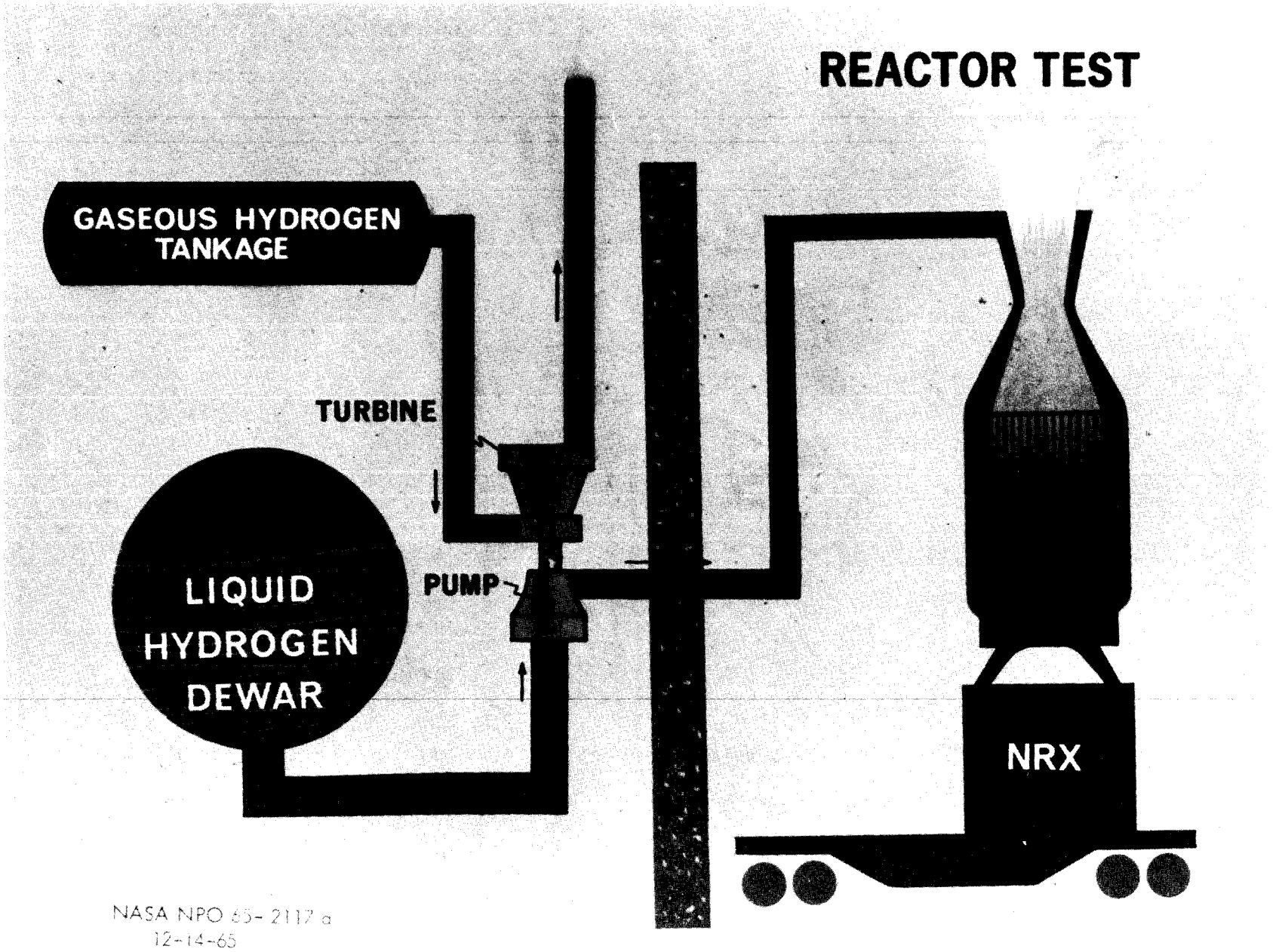
REACTOR TEST
GASEOUS HYDROGEN TANKAGE
TURBINE
PUMP
LIQUID HYDROGEN DEWAR
NRX
NASA NPO 65-2117 a
12-14-65

FIGURE 6

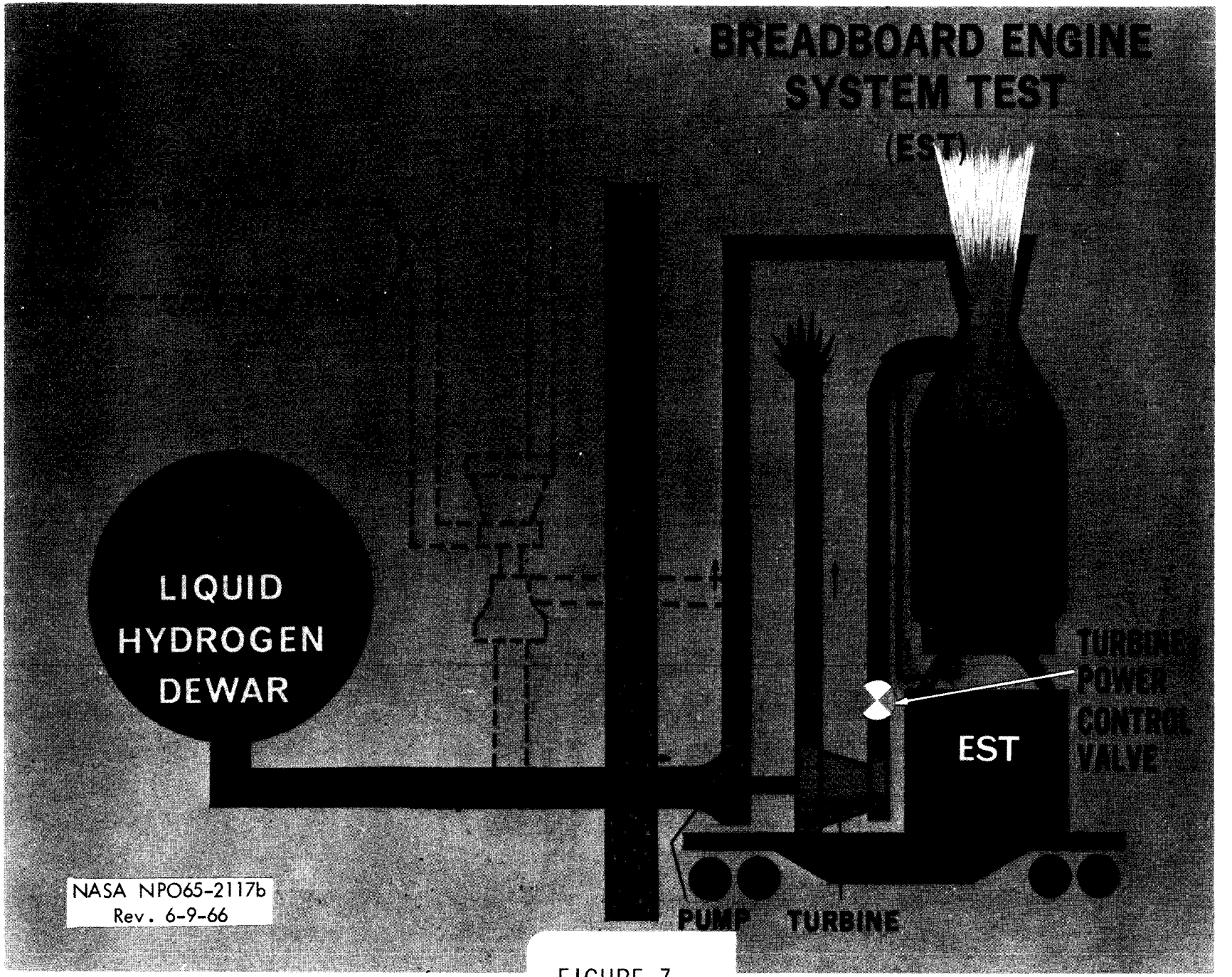
BREADBOARD ENGINE
SYSTEM TEST
(EST)
LIQUID
HYDROGEN
DEWAR
TURBINE
POWER
CONTROL
VALVE
EST
PUMP
TURBINE
NASA NPO65-2117b
Rev. 6-9-66

FIGURE 7

ENGINE SYSTEM TEST (EST)

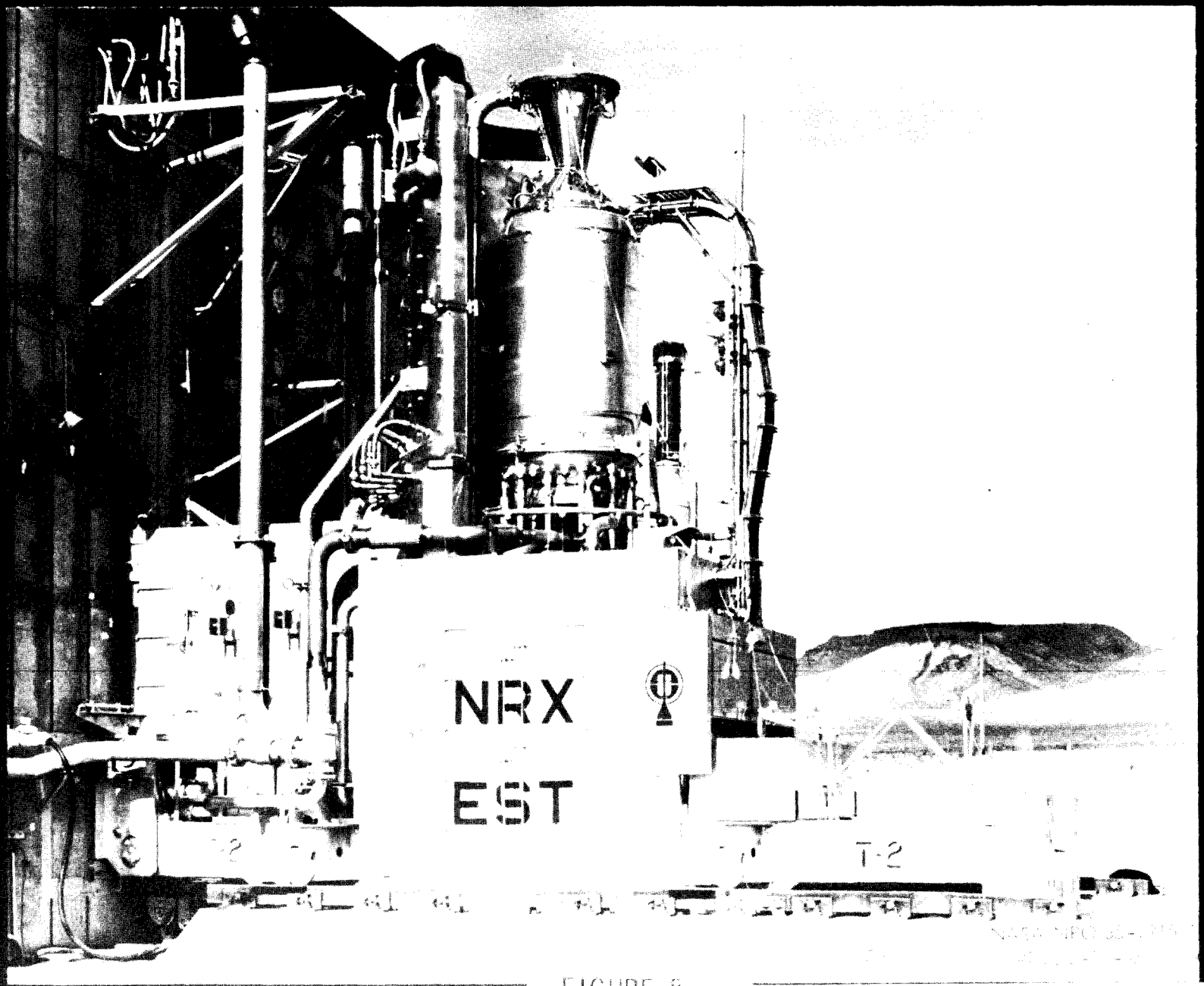

FIGURE 8

ENGINE SYSTEM TEST
PROPELLANT FEED SYSTEM INSTALLATION

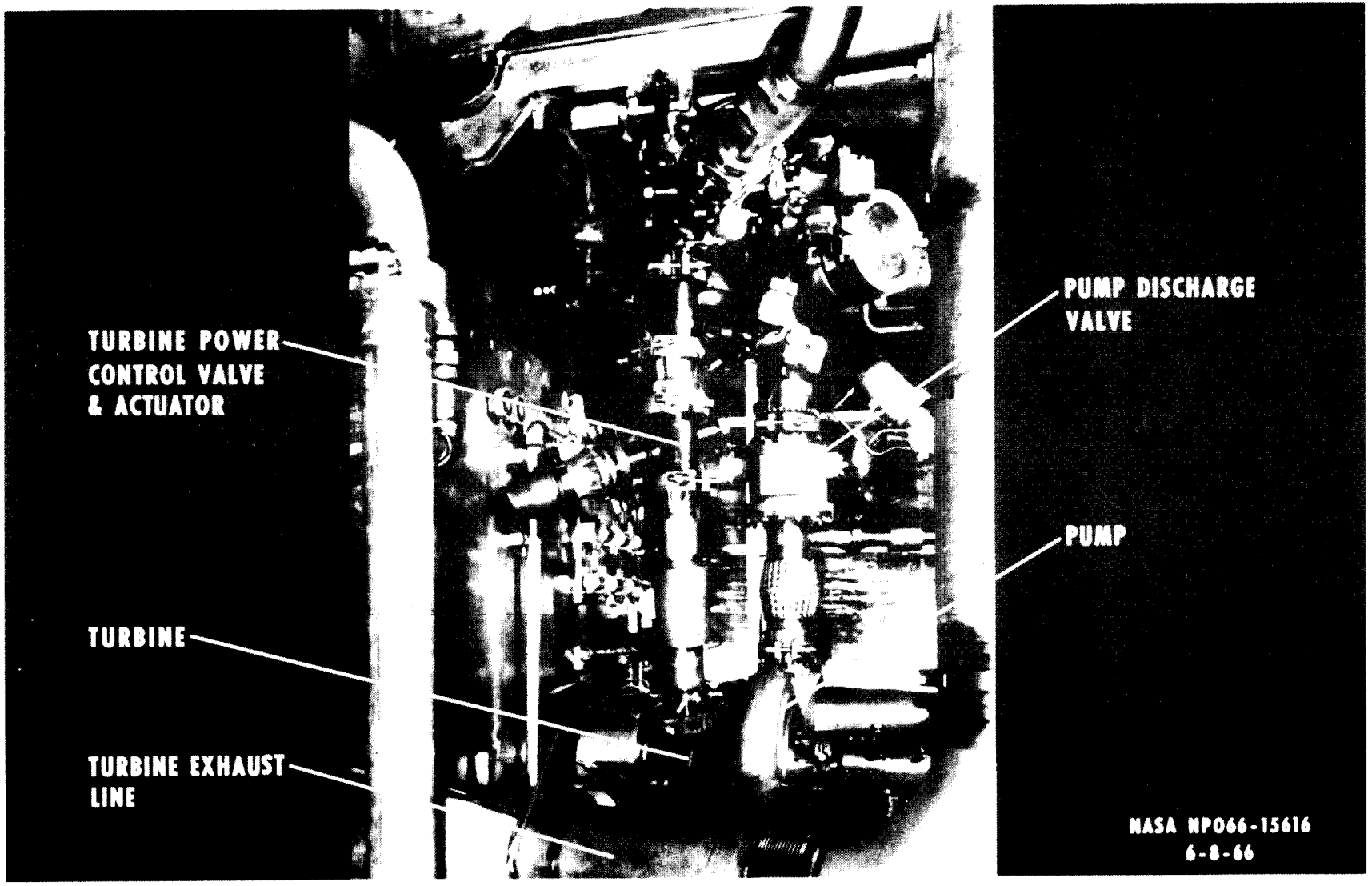

FIGURE 9

NERVA/EST TURBOPUMP

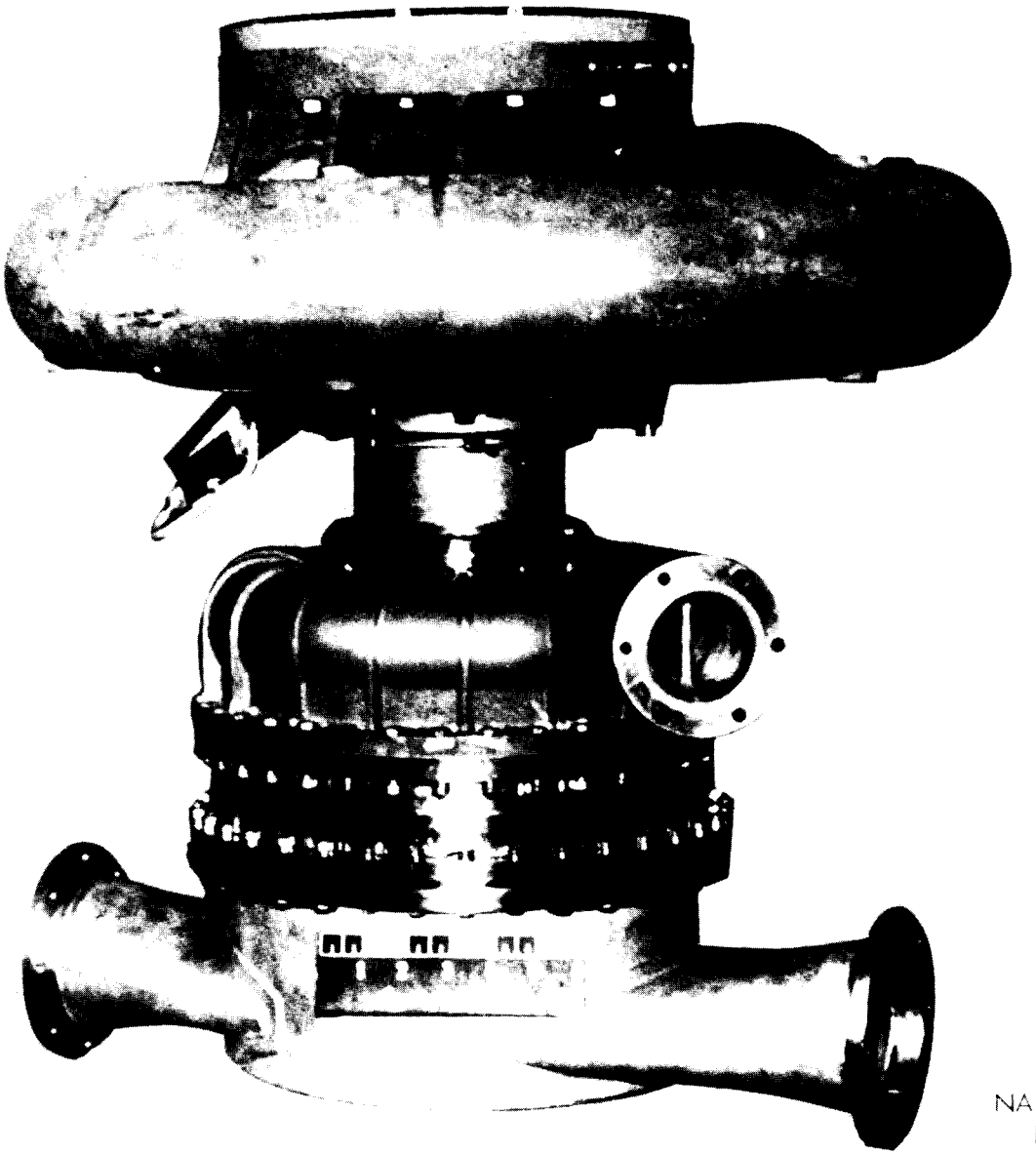

NASA NPO 64-669
REV. 1-24-66

FIGURE 10

HOT BLEED PORT NOZZLE - ENGINE SYSTEM TESTS

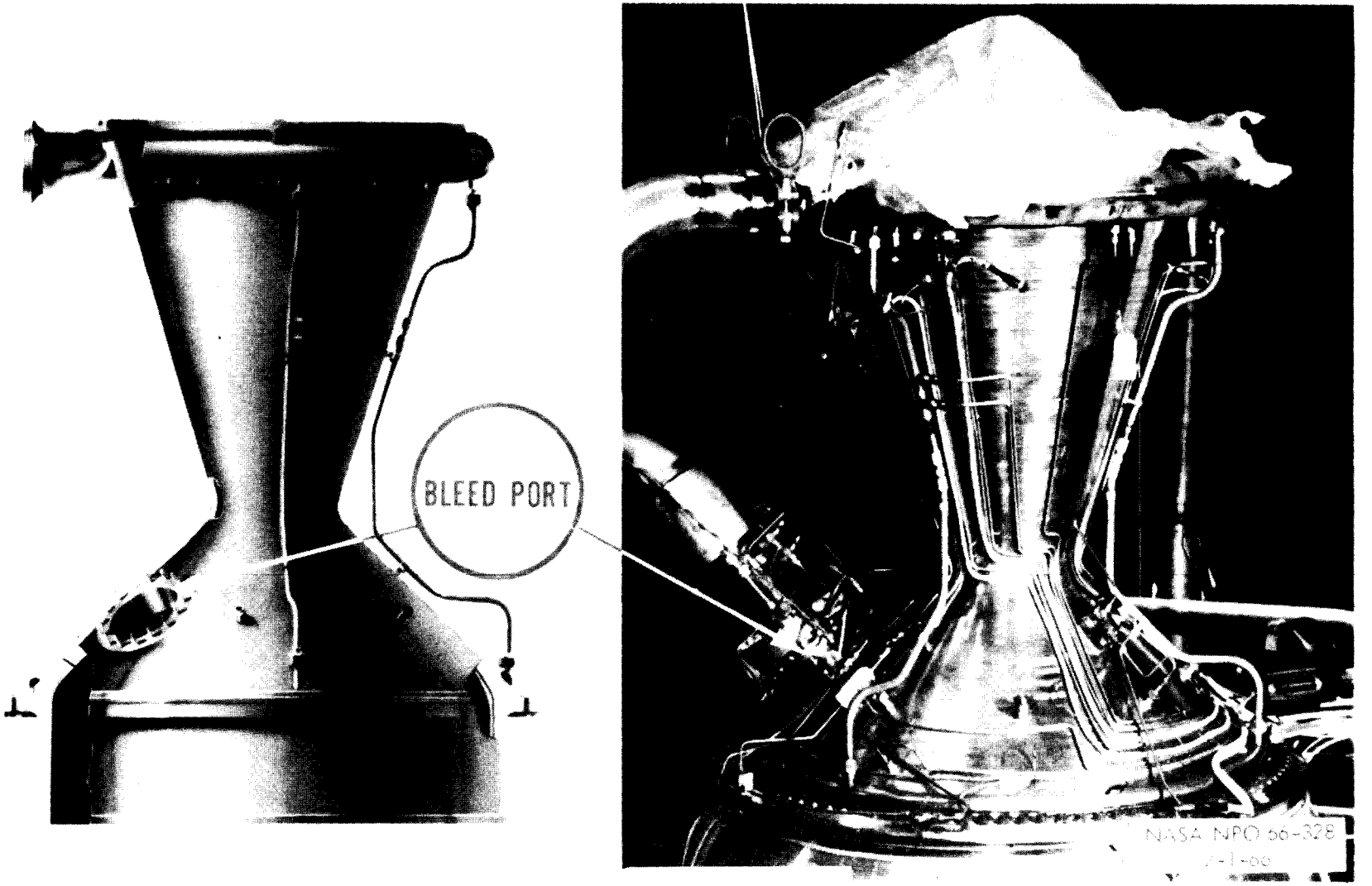

FIGURE 11

NUCLEAR ROCKET ENGINE CONTROL SCHEMATIC

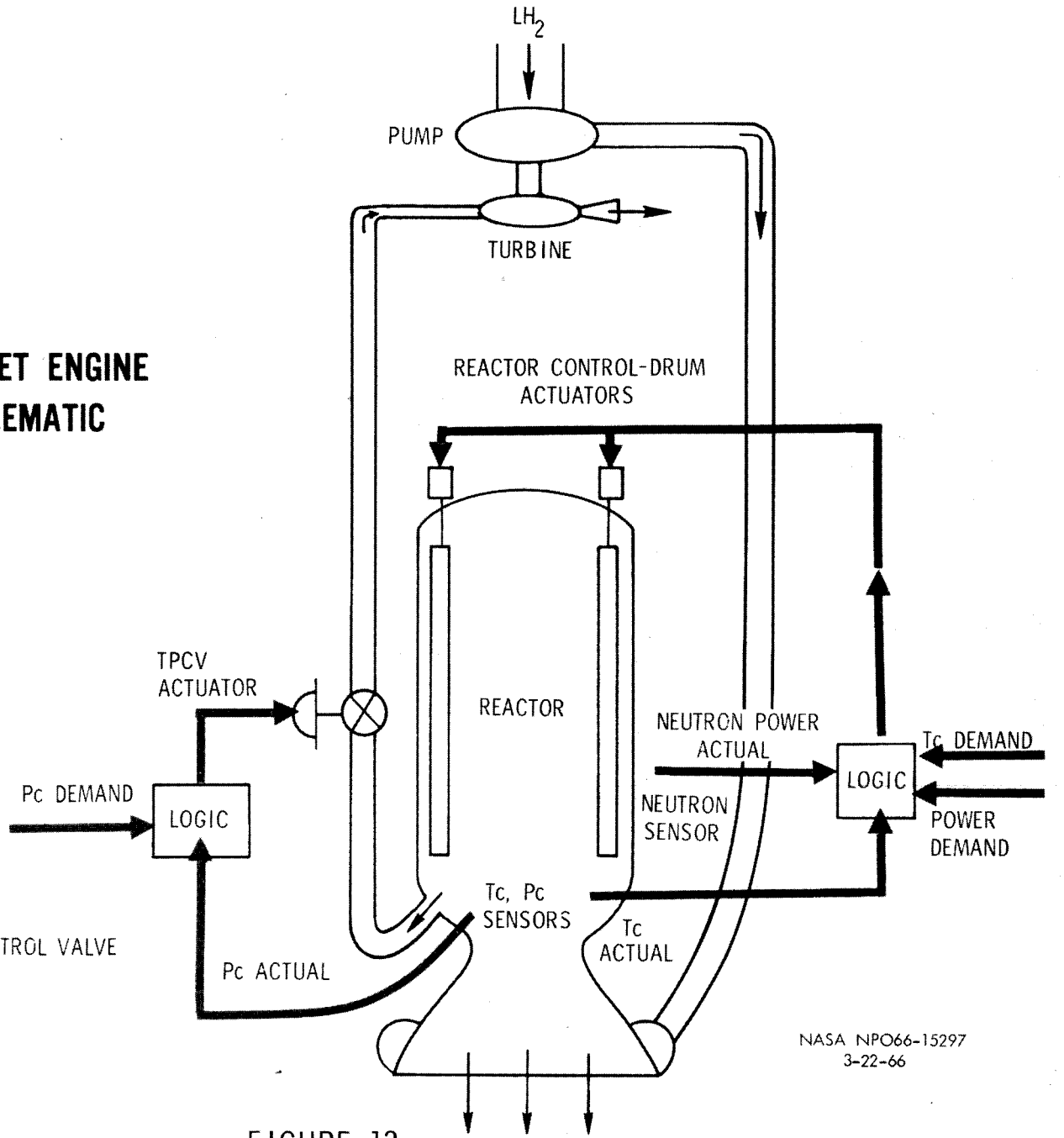

LEGEND:

TPCV: TURBINE POWER CONTROL VALVE

Tc: CHAMBER TEMPERATURE

Pc: CHAMBER PRESSURE

FIGURE 12

ENGINE SYSTEM TEST (EST)
SUMMARY OF POWER TESTS

DATE	START	POWER MW (MAXIMUM)	TEMPERATURE, ^{0}R (MAXIMUM)	DURATION MINUTES	PARTIAL LIST OF EXPERIMENTS
2/3/66	1	440	2550	11	NORMAL BOOTSTRAP TEMPERATURE RESPONSE
	2	250	2050	13	CHILLED REFLECTOR START TPCV RESPONSE TEMPERATURE LIMITER
2/11/66	3	230	2000	9	FIXED DRUM START CONTROL DRUM RESPONSE
	4	160	1450	-	LOW PRESSURE START (ABORT)
	5	350	2590	22	NORMAL START PRESSURE RESPONSE TEMPERATURE & POWER LIMITER CROSS LOOP LIMITER 2500 ^{0}R MAPPING NO FLUX-LOOP CONTROL
3/3/66	6	1090	4100	6	NORMAL START DESIGN POWER & TEMPERATURE
	7	1040	3690	15	NORMAL START 3400 ^{0}R MAPPING ON-OFF CONTROLLER
3/16/66	8	170	1500	-	CONTROL POSITIONING ERROR LED TO AUTOMATIC FLOW SHUTDOWN
	9	1090	4090	18	LOW PRESSURE START DESION POINT SYSTEM RESPONSE 4000 ^{0}R MAPPING
3/25/66	10	1130	4175	16	DURATION CAPABILITY DESIGN POINT SYSTEM RESPONSE
			TOTAL	110	(28 MINUTES NOMINAL FULL POWER)

NASA NPO 66-15342
REV. 9-27-66

FIGURE 13

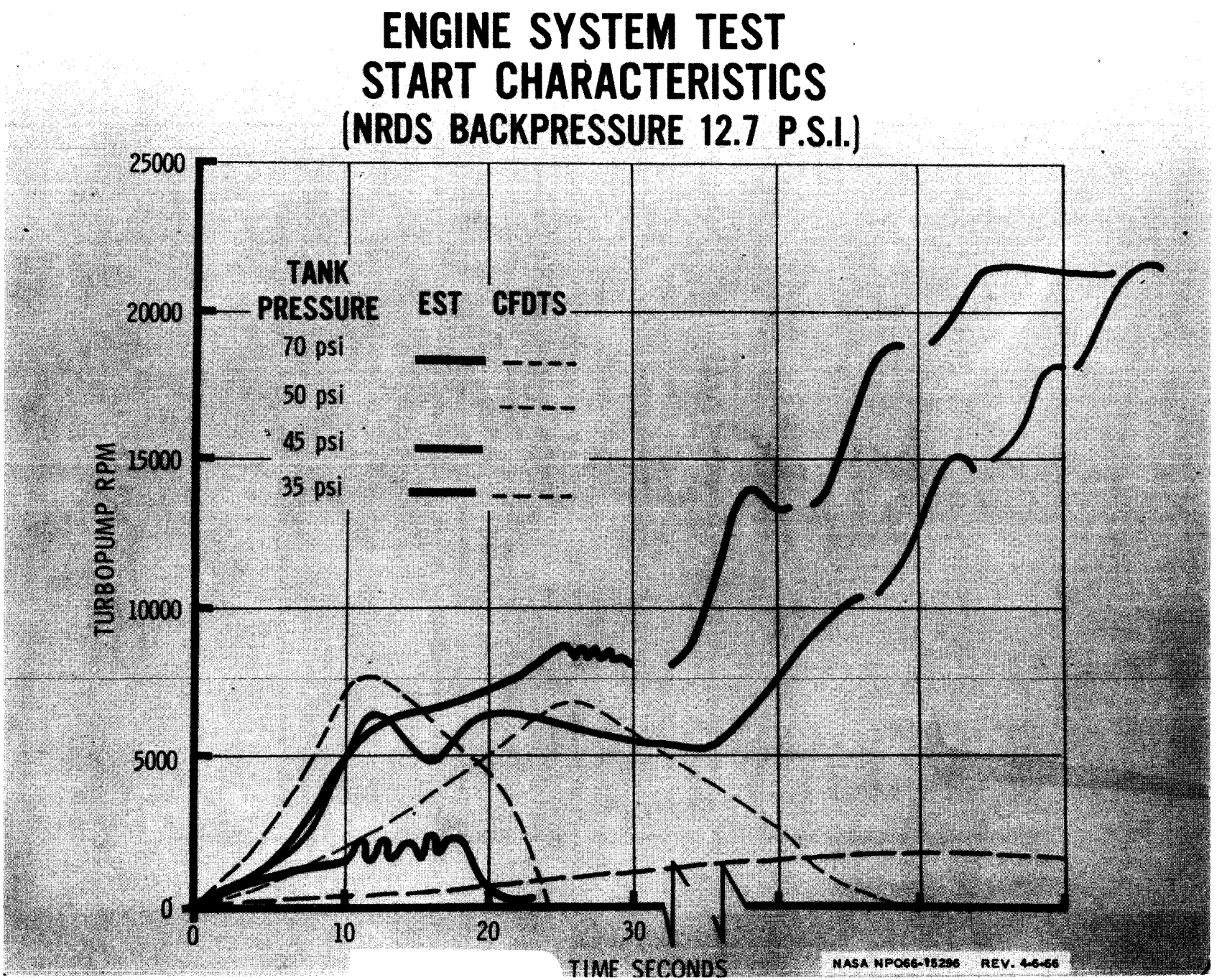
ENGINE SYSTEM TEST
START CHARACTERISTICS
(NRDS BACKPRESSURE 12.7 P.S.I.)
TANK PRESSURE
EST
CFDTS
70 psi
50 psi
45 psi
35 psi
TURBOPUMP RPM
25000
20000
15000
10000
5000
0
0
10
20
30
TIME SECONDS
NASA NPO66-15296 REV. 4-6-66

FIGURE 14

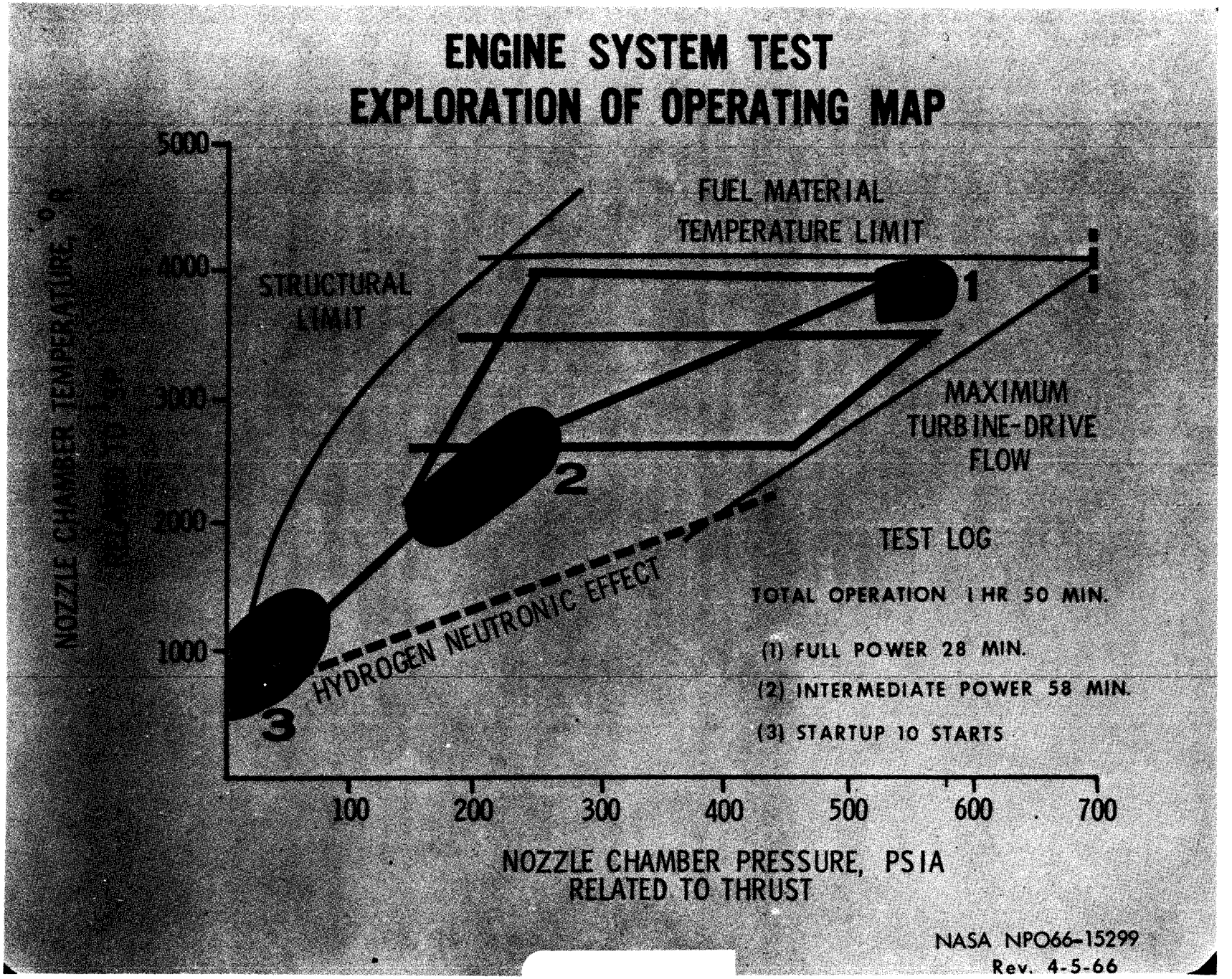
ENGINE SYSTEM TEST
EXPLORATION OF OPERATING MAP
NOZZLE CHAMBER TEMPERATURE, °R
5000
4000
3000
2000
1000
FUEL MATERIAL
TEMPERATURE LIMIT
STRUCTURAL
LIMIT
1
2
3
MAXIMUM
TURBINE-DRIVE
FLOW
HYDROGEN NEUTRONIC EFFECT
TEST LOG
TOTAL OPERATION 1 HR 50 MIN.
(1) FULL POWER 28 MIN.
(2) INTERMEDIATE POWER 58 MIN.
(3) STARTUP 10 STARTS
100
200
300
400
500
600
700
NOZZLE CHAMBER PRESSURE, PSIA
RELATED TO THRUST
NASA NPO66-15299
Rev. 4-5-66

FIGURE 15

NRX-A5 REACTOR

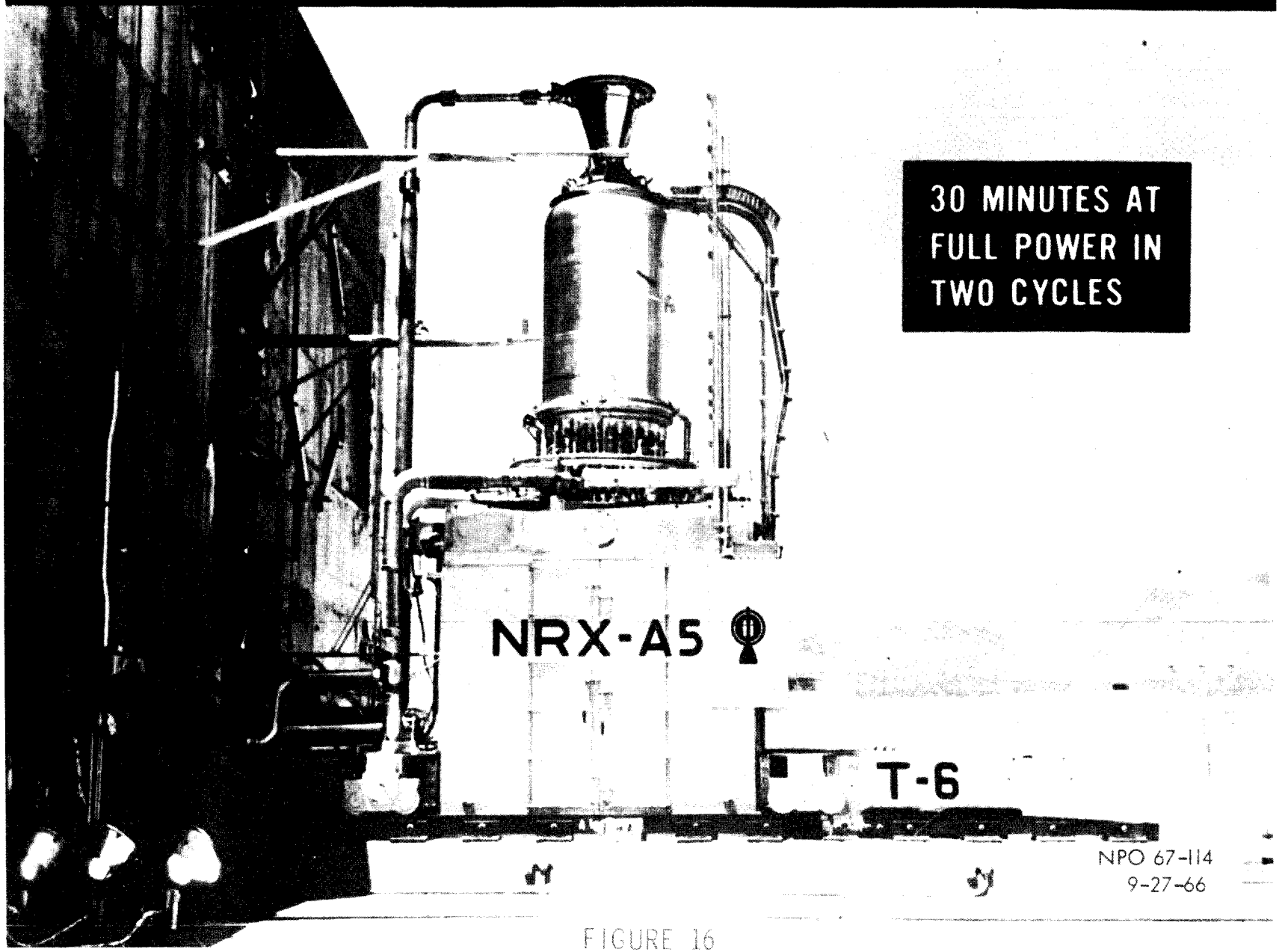

30 MINUTES AT FULL POWER IN TWO CYCLES

FIGURE 16

NERVA ENGINE

- THRUST
  200,000 - 250,000 LB
- POWER
  5,000 M.W.
- CHAMBER TEMPERATURE
  4,500°R
- SPECIFIC IMPULSE
  825 SEC
- CHAMBER PRESSURE
  625 PSIA

NASA NPO 67-49
9/27/66

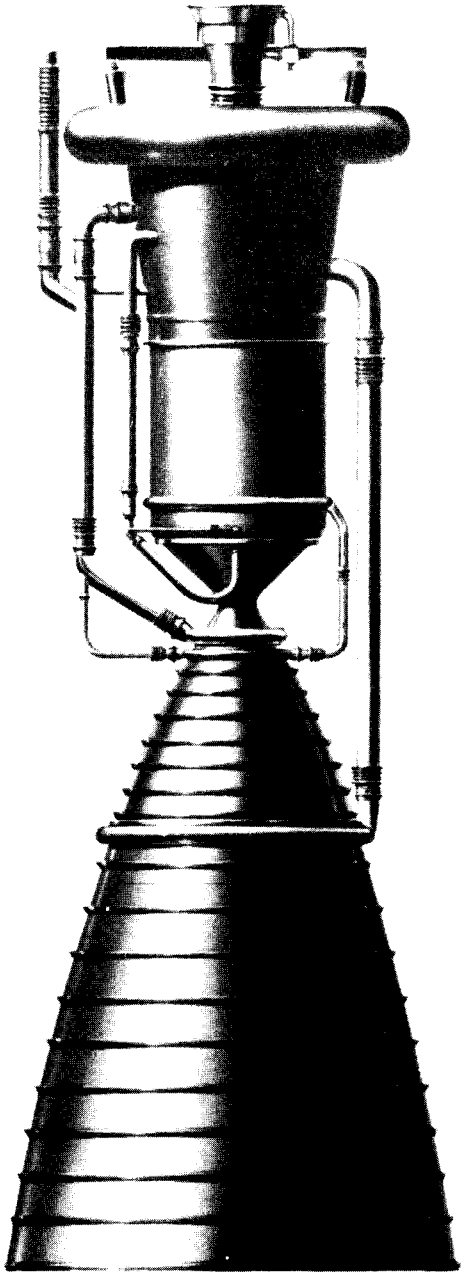

FIGURE 17